Accepted Manuscript

Analysis of oxidised and glycated aminophospholipids: Complete structural characterisation by C30 liquid chromatography-high resolution tandem mass spectrometry

Simone Colombo, Angela Criscuolo, Martin Zeller, Maria Fedorova, M. Rosário Domingues, Pedro Domingues

PII: S0891-5849(19)30356-9

DOI: https://doi.org/10.1016/j.freeradbiomed.2019.05.025

Reference: FRB 14286

To appear in: *Free Radical Biology and Medicine*

Received Date: 28 February 2019

Revised Date: 14 May 2019

Accepted Date: 22 May 2019

Please cite this article as: S. Colombo, A. Criscuolo, M. Zeller, M. Fedorova, M.Rosá. Domingues, P. Domingues, Analysis of oxidised and glycated aminophospholipids: Complete structural characterisation by C30 liquid chromatography-high resolution tandem mass spectrometry, *Free Radical Biology and Medicine* (2019), doi: https://doi.org/10.1016/j.freeradbiomed.2019.05.025.

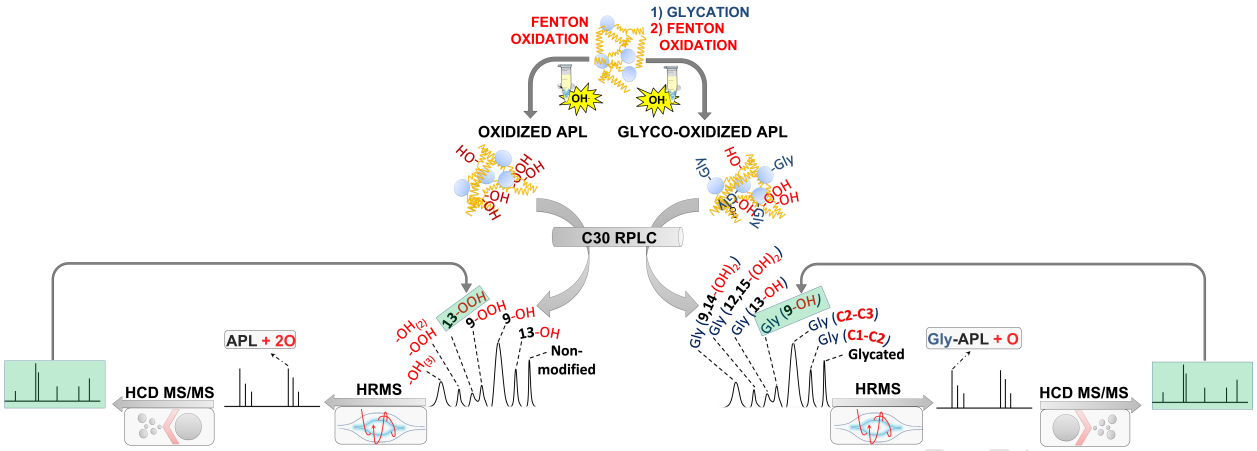

Analysis of oxidised and glycated aminophospholipids: complete structural characterisation by C30 liquid chromatography-high resolution tandem mass spectrometry

Simone Colombo[1], Angela Criscuolo[2,3,4], Martin Zeller[2], Maria Fedorova[3,4], M. Rosário Domingues[1,5], Pedro Domingues[1*]

[1]Mass Spectrometry Centre, Department of Chemistry & QOPNA, University of Aveiro, Campus Universitário de Santiago, 3810-193 Aveiro, Portugal

[2]Thermo Fisher Scientific, Hanna-Kunath-Straße 11, 28199 Bremen, Germany

[3]Institute of Bioanalytical Chemistry, Faculty of Chemistry and Mineralogy, Universität Leipzig,

[4]Center for Biotechnology and Biomedicine, Universität Leipzig, Germany

[5]Department of Chemistry & CESAM, University of Aveiro, Campus Universitário de Santiago, 3810-193 Aveiro, Portugal

Corresponding author: Pedro Domingues[1]

Lipidomic laboratory, Departamento de Química, Universidade de Aveiro, Campus Universitário de Santiago, 3810-193 Aveiro (PORTUGAL)

E-mail: p.domingues@ua.pt

Abstract

The aminophospholipids (APL), phosphatidylethanolamine (PE) and phosphatidylserine (PS) are widely present in cell membranes and lipoproteins. Glucose and reactive oxygen species (ROS), such as the hydroxyl radical ($^{\bullet}$OH), can react with APL leading to an array of oxidised, glycated and glycoxidised derivatives. Modified APL have been implicated in inflammatory diseases and diabetes, and were identified as signalling molecules in regulating cell death. However, the biological relevance of these molecules has not been completely established, since they are present in very low amounts, and new sensitive methodologies are needed to detect them in biological systems. Few studies have focused on the characterisation of APL modifications using liquid chromatography-tandem mass spectrometry (LC-MS/MS), mainly using C5 or C18 reversed phase (RP) columns. In the present study, we propose a new analytical approach for the characterisation of complex mixtures of oxidised, glycated and glycoxidised PE and PS. This LC approach was based on a reversed-phase C30 column combined with high-resolution MS, and higher energy C-trap dissociation (HCD) MS/MS. C30 RP-LC separated short and long fatty acyl oxidation products, along with glycoxidised APL bearing oxidative modifications on the glucose moiety and the fatty acyl chains. Functional isomers (e.g. hydroxy-hydroperoxy-APL and tri-hydroxy-APL) and positional isomers (e.g. 9-hydroxy-APL and 13-hydroxy-APL) were also discriminated by the method. HCD fragmentation patterns allowed unequivocal structural characterisation of the modified APL, and are translatable into targeted MS/MS fingerprinting of the modified derivatives in biological samples.

Keywords: phosphatidylethanolamine, phosphatidylserine, oxidation, glycation, mass spectrometry, lipidomics

Introduction

The aminophospholipids (APL), phosphatidylethanolamine (PE) and phosphatidylserine (PS), are main constituents of mammalian cell membranes and lipoproteins, displaying both structural and signalling functions [1]. Upon oxidative stress, reactive oxygen species (ROS) such as the hydroxyl radical ($^{\bullet}$OH), mediate the oxidation of APL, resulting in radical oxidation of unsaturated lipids fatty acyl chains and polar heads with the formation of oxygenated derivatives and truncation products, overall leading to a plethora of new oxidized or glycated/glycoxidised molecular species [2–6].

Oxidised APL might lose the activity of the non-modified precursor or acquire new biological functions. Oxidised PE and PS are known to be involved in critical events, such as cell death and the regulation of the inflammatory response. For example, it is known that hydroperoxy-PE derivatives are involved in the mediation of ferroptotic cell death [7]. Also, oxidised PS, including long chain oxidation products such as hydroxy-PS and hydroperoxy-PS, contribute to apoptotic cell recognition by macrophages [8,9]. Oxidised PE has been associated with a pro-inflammatory phenotype in human peripheral blood [10,11]. The role of oxidised PS in inflammation was also described and was related to both pro-inflammatory and anti-inflammatory outcomes [11,12,13]. Both oxidised PE and PS were detected *in vivo* in various diseases. For example, mono-oxygenated PE derivatives were detected in fibrocystic bronchoalveolar lavage in humans [14], and on activated platelets, monocytes [15], and macrophages [16]. Hydroxy-PS, hydroperoxy-PS and hydroxy-hydroperoxy-PS were also detected in post-mortem human brains with Alzheimer's disease [17], whereas PS oxidised on the polar head were found in human keratinocytes stimulated with oxidative stress [18].

Due to the presence of a free amino group in the polar head, APL are also prone to form covalent adducts with glucose [19]. Once formed, glycated APL can be further oxidised, leading to glycoxidised APL, also known as advanced glycoxidation end products (AGE) [20,21]. Some

authors reported that glycated and glycoxidised PE promotes lipid peroxidation via generation of ROS [21,22]. Similarly to oxidized PE, glycated and glycoxidised PE were found to promote an inflammatory phenotype in peripheral blood [10,23]. Glycated and glycoxidised PE have also been identified as factors modulating the expression of several proteins in rat cardiomyocytes [21]. Glycated PE was detected in the plasma of patients associated with hyperglycemic conditions [19,22]. Glycated and glycoxidised PE were also detected in red blood cells and plasma samples from healthy and diabetic subjects [19,22,24–28], in diabetic rats [29], and mitochondrial membranes of several mammalian species [30]. However, mostly because of their low abundance *in vivo*, the potential of oxidised, glycated and glycoxidised APL as biomarkers for disease is still far from being clarified and deserves to be explored.

Several studies suggest that there is a structure-activity relationship for oxidised PE and oxidised PS [7,8,10,14,15]. Indeed, the detection of specific isomers of modified APL in inflammatory diseases could confirm their role in the disease pathogenesis, validate biomarkers for early diagnosis, and highlight new targets for drug development. Thus, there is a need to develop sensitive and selective liquid chromatography-tandem mass spectrometry (LC-MS/MS) platforms that can lead to a more detailed characterisation of modified APL in complex mixtures or matrices. As reviewed elsewhere, LC-MS/MS has been widely used to characterise oxidised PC [4,5], but little work has been done to investigate modified PE [31–35] and modified PS [36,20,37]. In studies reporting the LC-MS/MS analysis of oxidised PE and PS, columns packed with C5 [20,32,37], and C18 [27,15,38,28,14] were the most commonly employed. The first application of a C30 column for the analysis of APL was proposed by Houjou and co-authors [39], which have identified 110 species (PC, PE, PI and PS) from rat liver. More recently, C30 columns were successfully employed in the lipidomic analyses of human plasma [40], rat plasma and rat liver [41]. C30 reversed phase (RP) LC has not yet been used to study modified APL. In the present study, we propose an LC-MS/MS approach based on C30 RP-LC, high-resolution MS identification and

higher energy C-trap dissociation (HCD) MS/MS for the analysis of the oxidised, glycated and glycoxidised derivatives of four different APL standards – two from the PE class and two from the PS class. This method, herein tested for the first time on complex mixtures of modified APL, could separate positional and functional isomers of oxidised, glycated and glycoxidised PE and PS, which showed characteristic HCD-type fragmentation patterns for each group of modified derivatives.

Materials and Methods

Reagents / chemicals

Phospholipid standards 1-palmitoyl-2-oleoyl-*sn*-3-glycerophosphoethanolamine (POPE), 1-palmitoyl-2-linoleoyl-*sn*-3-glycerophosphoethanolamine (PLPE), 1-palmitoyl-2-oleoyl-*sn*-3-glycerophosphoserine (POPS) and 1-palmitoyl-2-linoleoyl-*sn*-3-glycerophosphoserine (PLPS) were purchased from Avanti Polar Lipids, Inc. (Alabaster, AL, USA) and used without further purification. Acetonitrile, isopropanol, water, methanol, ammonium formate (Optima^{TM} LC/MS grade) and chloroform (LC-MS grade) were obtained from Fisher Scientific (Schwerte, Germany). Formic acid (LC-MS grade) was purchased from Sigma-Aldrich (Sigma-Aldrich, Munich, Germany). $FeCl_2$ and hydrogen peroxide (H_2O_2) (30%, w/v) used for the Fenton reaction were acquired from Merck (Darmstadt, Germany). Glucose and ammonium bicarbonate were purchased from Sigma-Aldrich (Saint Louis, MO, USA).

Phospholipid glycation and oxidation

Glycated PL samples were synthesised by adding to 1.2 mg of glucose, dissolved in 150 µL of methanol, to 0.5 mg of dry PL. The solution was mixed thoroughly, and the reaction glass was introduced in boiling H_2O with continuous magnetic stirring, for 45 minutes [33,37].

Non-modified and glycated phospholipids were oxidised by Fenton reaction. Briefly, 125 µg of phospholipid previously dried under nitrogen stream were resuspended in 62.5 µL ammonium bicarbonate buffer (pH 7.4) containing 50 mM H_2O_2 and 40 µM $FeCl_2$. The suspension was incubated in the dark at 550 RPM, 37 °C, during 48 h. Phospholipids were analysed by C30 RP-LC-MS/MS after 24h and 48h from the beginning of the Fenton reaction. For the detailed experimental procedures of PL oxidation, the reader is referred to previously published works in which the same protocol was applied [11,37].

C30 RP-LC-MS/MS

The oxidation, glycation and glycoxidation products were analyzed by RP-LC-MS/MS performed on a Thermo Fisher Scientific UltiMate3000™ UHPLC system (Thermo Fisher Scientific, Germering, Germany) coupled to a Q Exactive™ HF hybrid quadrupole-Orbitrap mass spectrometer (Thermo Fisher Scientific, Bremen, Germany) using the conditions recently reported by Criscuolo *et al*, with slight modifications [42]. The reaction mixture was diluted in methanol to the final concentration of 250 ng/µL, and 5 µL of this solution were introduced into an Accucore™ C30 column (150 x 2.1 mm) equipped with 2.6 µm diameter fused-core particles (Thermo Fisher Scientific, Germering, Germany). The mobile phases consisted of H_2O /acetonitrile 50/50 v/v with 0.1% formic acid and 5 mM ammonium formate (phase A), and isopropanol/acetonitrile/ H_2O 85/10/5 v/v/v with 0.1% formic acid and 5 mM ammonium formate (phase B). The solvent gradient was set up with an initial ramp from 10% B to 86% B at 20 min, followed by a linear increase to 95% B at 22 min, which was isocratically held for 4 minutes. The percentage of B was decreased to 10% at minute 26.1 and maintained isocratically until the end of the run at minute 32. The flow rate was 300 µL/min.

During full MS experiments, the Q Exactive™ HF hybrid quadrupole-Orbitrap mass spectrometer operated on a mass range comprised between *m/z* 400 and *m/z* 1600, with a 120000 resolution setting, an injection time of 100 ms and an AGC target of $1E^6$, in positive (electrospray

voltage +3.5 kV) and negative (electrospray voltage -3.5 kV) ion modes, through a polarity switching method. The capillary temperature was 230 °C, the vaporiser temperature was 300 °C, the S-Lens RF level was at 35%, and the sheath gas and the auxiliary gas flows were respectively 45 arbitrary units (AU) and 15 AU.

Tandem mass spectra of $[M+H]^+$ and $[M-H]^-$ precursor ions were generated through polarity switching and HCD fragmentation, with cycles consisting of one full scan mass spectrum plus five data-dependent MS/MS, scans for each mode, with an isolation window of 1 *m/z*, a dynamic exclusion of 10 seconds and an intensity threshold of $3.3E^4$. Normalised collision energy™ (NCE) was stepped between 10, 20 and 30 eV. The instrument operated with the resolution setting of 15000, an injection time of 150 ms and an AGC target of $1E^5$ throughout all the MS/MS acquisitions.

Results

In this work, we have analysed oxidised PLPE, PLPS, POPE and POPS, and their glycated derivatives by reversed-phase liquid chromatography with high-resolution MS, and HCD MS/MS fragmentation detection using a C30 LC column (C30 LC-MS). Lipid species were oxidised by $^{\bullet}OH$ generated under Fenton reaction, as reported in previous studies [11,37]. Several types of oxidation and glycoxidation products were analysed for the first time using C30 LC-MS and characterised by HCD MS/MS. These oxidation and glycoxidation products included long chain products (mono-, di- and tri-oxygenated derivatives), short chain products (APL esterified with oxononanoic and azelaic acid), and glycoxidised APL with polar head oxidation, i.g, APL adducted to end products of glucose oxidation [44]. All the modified APL analysed in the present study were summarised in Table 1.

Table 1. The ion identities, measured (Exp *m/z*), theoretical masses (Theo *m/z*), mass measurement errors (Error ppm) and retention time (RT) for the oxidation and glycoxidation products of PE and PS analysed by C30 LC-MS.

	Phosphatidylethanolamine (X=E)				Phosphatidylserine (X=S)			
Derivative	Exp *m/z* $[M+H]^+$	Theo *m/z* $[M+H]^+$	Error [ppm]	RT [min]	Exp *m/z* $[M+H]^+$	Theo *m/z* $[M+H]^+$	Error [ppm]	RT [min]
PLPX-(9-OH)	732.517	732.518	-1.4	14.0	776.506	776.508	-2.6	12.8
PLPX-(13-OH)	732.517	732.518	-1.4	13.8	776.506	776.508	-2.6	12.6
PLPX-(9-OOH)	748.511	748.513	-2.7	13.1	792.501	792.503	-2.5	9.9
PLPX-(12-OOH)	748.511	748.513	-2.7	12.8				
PLPX-(13-OOH)					792.501	792.503	-2.5	9.6
PLPX-(9-OH,14-OH)	748.511	748.513	-2.7	11.3	792.501	792.503	-2.5	10.3
PLPX-(12-OH,15-OH)	748.511	748.513	-2.7	11.1	792.501	792.503	-2.5	10.3
PLPX-(13-OH,15-OH)	748.511	748.513	-2.7	11.1				
PLPX-(9-OH,12-OH,15-OH)	764.506	764.508	-2.6	9.6	808.496	808.498	-2.5	8.6
PLPX-(9-OH,12-OOH)	764.506	764.508	-2.6	11.2	808.496	808.498	-2.5	10.3
PLPX-(9-OOH,12-OH)	764.506	764.508	-2.6	11.2	808.496	808.498	-2.5	10.3
POPX-(8-OH)	734.532	734.534	-2.7	13.4				
POPX-(9-OH)	734.532	734.534	-2.7	14.8	778.522	778.523	-1.3	13.6
POPX-(10-OH)	734.532	734.534	-2.7	14.8	778.522	778.523	-1.3	13.6
POPX-(8-OOH)	750.527	750.529	-2.7	13.8	794.517	794.518	-1.3	12.3
POPX-(9-OOH)	750.527	750.529	-2.7	13.8	794.517	794.518	-1.3	12.3
PONPX	608.391	608.393	-3.3	8.8	652.381	652.383	-3.1	7.5
PAzPX	624.386	624.388	-3.2	8.1	668.375	668.377	-3.0	6.9
Glycated PLPX	878.576	878.576	0.0	17.4	922.565	922.566	-1.1	15.8
Formyl-PLPX	744.518	744.518	0.0	16.3				
Carboxymethyl-PLPX	774.528	774.529	-1.3	16.2				
Glycated PLPX-(9-OH)	894.570	894.571	-1.1	14.6				
Glycated PLPX-(13-OH)	894.570	894.571	-1.1	14.3				
Glycated PLPX-(9-OH,14-OH)	910.565	910.566	-1.1	11.1				
Glycated PLPX-(12-OH,15-OH)	910.565	910.566	-1.1	11.6				
Glycated POPX	880.591	880.592	-1.1	18.1	924.581	924.581	0.0	16.8
Formyl-POPX	746.534	746.533	1.3	17.3	790.523	790.523	0.0	17.0
Carboxymethyl-POPX	776.544	776.544	0.0	17.2	820.534	820.534	0.0	14.6
Glycated POPX-(9-OH)	896.586	896.586	0.0	15.4				
Glycated PONPX	770.446	770.446	0.0	8.5				
Glycated PAzPX	786.440	786.440	0.0	7.8	830.430	830.430	0.0	6.2

Separation of oxidised derivatives of APL by C30 LC and characterisation by MS and HCD MS/MS

A comparison of the total LC-MS base peak chromatograms of the oxidised APL is depicted in Figure 1. Non-modified APL eluted at the highest RT, between 15.1 - 17.5 min. Modified APL showed different elution profiles and eluted at lower RT when compared with non-modified APL:

Mono-hydroxy derivatives (APL+O, mass shift: + 15.995 Da) eluted with an RT between 12.9 - 14.9 min, hydroperoxy and di-hydroxy derivatives (APL+2O, mass shift: +31.990 Da) eluted between 10.1 and 13.6 min, hydroxy-hydroperoxy and tri-hydroxy derivatives (APL+3O, mass shift: + 47.985 Da), observed only in ox-PLPS and ox-PLPE, eluted between at 8.6 min and 11.3 min. Short chain oxidation products were also only observed in ox-PLPS and ox-PLPE, as previously reported [32,33,45]. These short chain derivatives, esterified to an oxidatively cleaved *sn*-2 fatty acid chain, eluted with the lowest RT, between 6.5 min and 8.0 min (azelaoyl derivative at 6.9 min and 9-oxo-nonanoyl derivative at 7.5 min). Non-modified APL esterified to linoleic acid, along with their hydroxy, di-hydroxy and hydroperoxy derivatives, eluted on average 1.05 minutes before the correspondent species esterified to oleic acid.

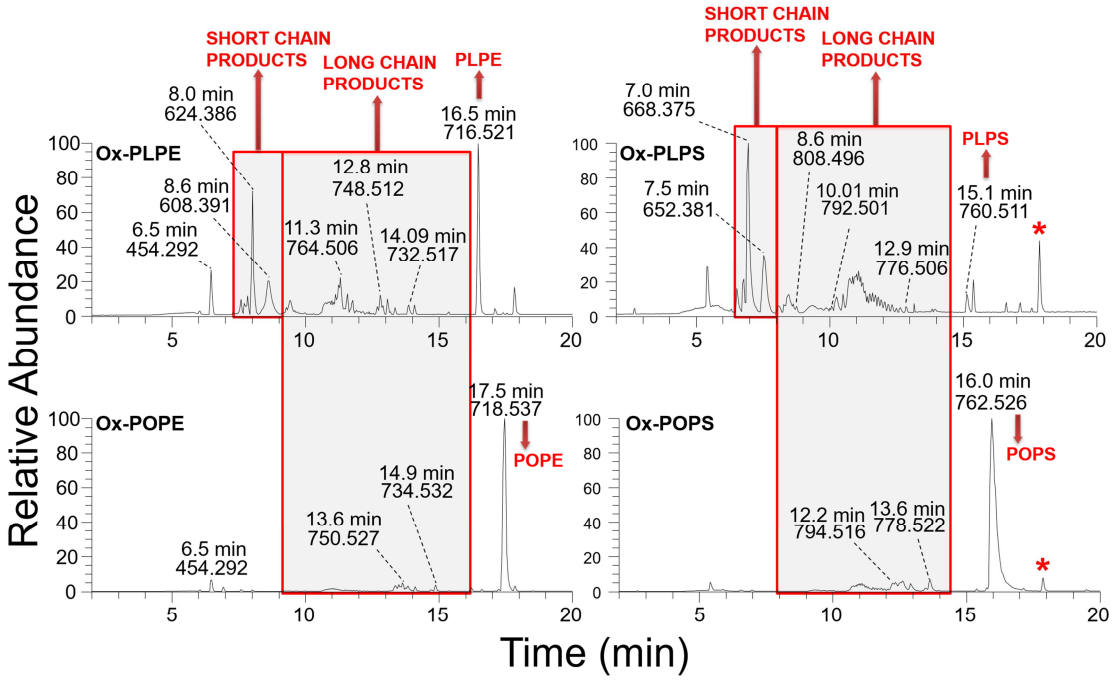

Figure 1. Comparison of the LC-MS base peak profiles of PLPE, PLPS, POPE and POPS subjected to Fenton reaction for 24 h, acquired in positive ion mode. *Uncharacterized impurities eluting at 18 min.

The extracted ion current (XIC) chromatograms of PLPS and its main oxidation products, acquired in positive ion mode, were plotted in Figure 2 as an example. As depicted in Figure 2, the

XIC chromatograms plotted for each *m/z* of interest often resulted in more than one peak, suggesting the presence of functional and positional isomers. Whenever the separation of these isomers was possible using C30 LC, the HCD MS/MS spectra for each isomer were acquired, thus enabling the analysis of their characteristic fragmentation patterns and the identification of common and specific product ions.

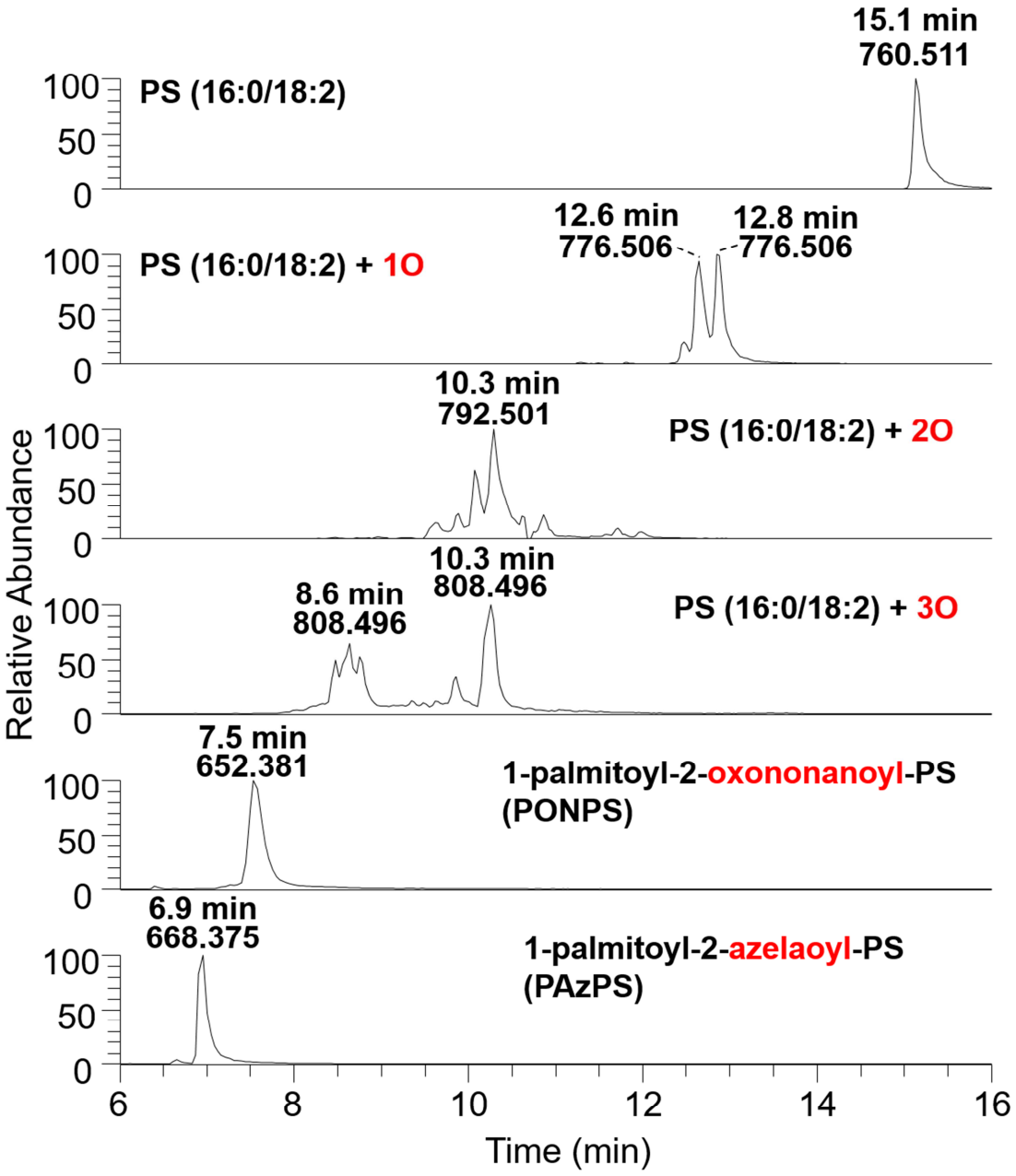

Figure 2. XIC chromatograms (± 5 ppm) of PLPS and its main oxidation products acquired in positive ion mode.

Identification and structural characterisation of different isomers of oxidised APL by HCD-MS/MS

Oxygenated products having the same elemental composition, namely positional or functional isomers, showed different retention on the C30 column. HCD MS/MS data acquired in positive ion mode provided information about the type of oxygenated moieties and their position on the fatty acyl chains. HCD MS/MS acquired in negative ion mode are not described in this manuscript, since no additional information could be obtained.

The hydroxy-PLPS ($[M+H]^+$, *m/z* 776.506) eluted in two major peaks at 12.6 and 12.8 min, corresponding to different positional isomers (Figure 2). The MS/MS spectra of the two isomers (Figure 3), showed ions arising from the neutral loss (NL) of water (18 Da), and combined NL of water and the phosphoserine polar head (185+18 Da=203 Da) (Table 2).

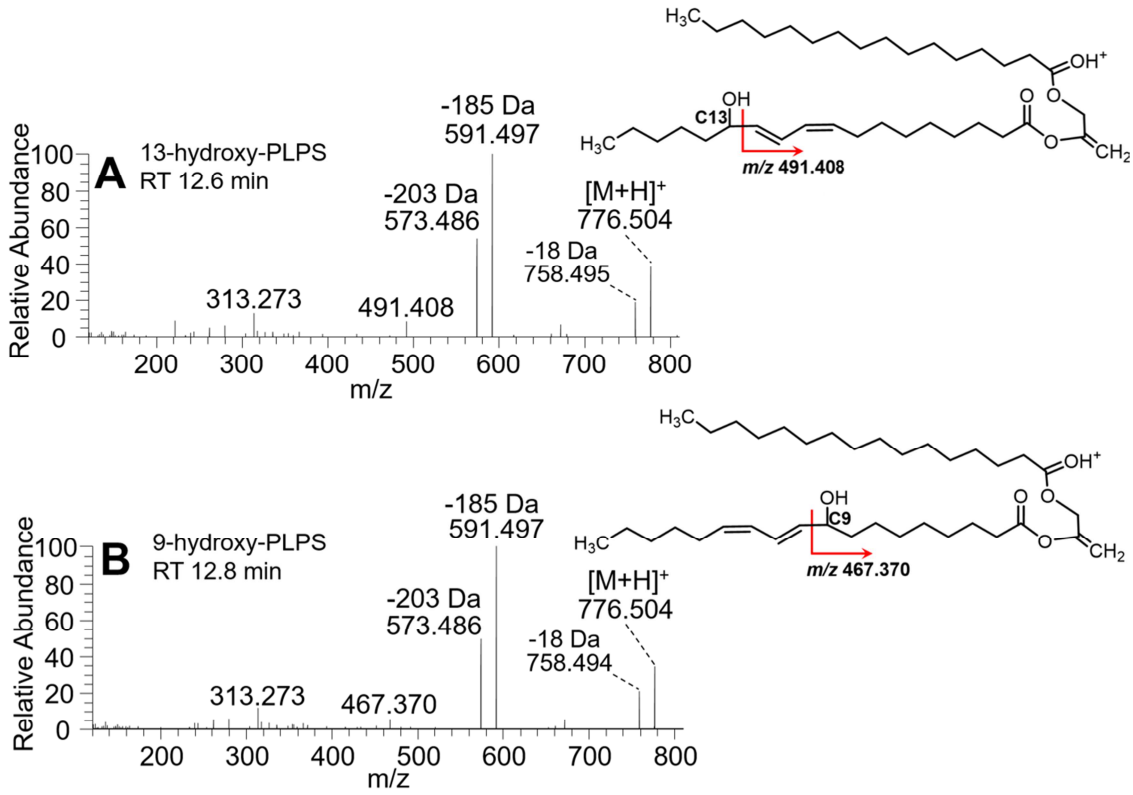

209

210 **Figure 3**. HCD MS/MS spectra and proposed fragmentation pathways of hydroxy-PLPS
211 isomers ($[M+H]^+$, *m/z* 776.506) that eluted at 12.6 min (A) and 12.8 min (B).

212 In the MS/MS spectra of PLPS+O acquired at 12.6 min (Figure 3A), it is possible to see a
213 minor diagnostic product ion at *m/z* 491.409 indicating the insertion of the hydroxy group at C-13
214 (13-hydroxy-PLPS isomer); in the MS/MS spectrum of PLPS+O at 12.8 min (Figure 3B), the minor
215 product ion at *m/z* 467.370 pinpointed the hydroxy group at C-9 (9-hydroxy-PLPS isomer). Product
216 ions observed at *m/z* 491.409 and *m/z* 467.370 resulted from the cleavage between the carbon
217 bearing the hydroxy functional group and the unsaturated carbon in vinylic position, after the NL of
218 the polar head (185 Da) [23,32].

219 Hydroxy-PLPE derivatives ($[M+H]^+$, *m/z* 732.517) eluted in two major peaks at RT 13.8 min
220 and 14.0 min (Supplementary Figure 1). Both MS/MS spectra showed the NL of water (18 Da), NL
221 of phosphoethanolamine (141 Da) and the combined NL of water and the phosphoethanolamine
222 polar head (141+18 Da) (Table 2). In the MS/MS spectra, it was also possible to observe the

223 diagnostic product ions that suggested the formation of the 13-hydroxy-PLPE (*m/z* 491.409) and 9-
224 hydroxy-PLPE (*m/z* 467.368) isomers, respectively for the isomers that eluted at 13.8 min and 14.0
225 min (Supplementary Figure 4), as observed for PLPS.

226 Besides positional isomers, oxidation of APL can also lead to the formation of functional
227 isomers, which occurred for poly-oxygenated APL. PLPS+2O derivatives ($[M+H]^+$, *m/z* 792.491)
228 eluted in two minor peaks at RT 9.6 and 9.9 min, and one major peak at RT 10.3 min (Figure 1).
229 The MS/MS spectra acquired at 9.6 min and 9.9 min showed the NL of the serine polar head (185
230 Da) and the combined NL of the polar head and water (203 Da) (Figure 4). In both MS/MS spectra,
231 it was possible to observe the NL of water (18 Da) and the NL of H_2O_2 (34 Da), which confirmed
232 the presence of the hydroperoxy moiety. The minor diagnostic product ions at *m/z* 491.410 (Figure
233 4A) and *m/z* 467.368 (Figure 4B) indicated that the compounds eluting at RT 9.6 min and 9.9 min
234 were modified by a hydroperoxy moiety at C-13 and C-9, respectively. The MS/MS spectrum of
235 PLPS+2O at 10.3 min (Figure 4C) showed the NL of 185 Da, combined NL of water and
236 phosphoserine (203 Da), and multiple NL of water molecules (18 Da and 36 Da), which overall
237 indicated the presence of a di-hydroxy-PLPS (Table 2). Additionally, the minor diagnostic product
238 ions observed at *m/z* 507.403 and *m/z* 467.372 indicated the presence of the isomers 12,15-
239 dihydroxy-PLPS and 9,14-dihydroxy-PLPS, respectively, coeluting at RT 10.3 min.

240 POPS+2O ($[M+H]^+$, *m/z* 794.518) eluted in one broad peak at 12.3 min (Supplementary
241 Figure 2). The MS/MS spectrum showed the NL of H_2O_2 (34 Da), which confirmed the formation
242 of a hydroperoxy derivative (hydroperoxy-POPS), and a product ion formed by the combined NL of
243 H_2O_2 and phosphoserine (219 Da), as base peak (Table 2, Figure 4D). This intense NL of 219 Da
244 was not observed in the MS/MS spectra of hydroperoxy-PLPS (Figures 4A, 4B), nor in the MS/MS
245 spectra of di-hydroxy-PLPS (Figure 4C). The minor diagnostic product ions at *m/z* 453.538 and *m/z*
246 467.372 indicated the coelution of two positional isomers, 8-hydroperoxy-POPS and 9-hydroperoxy
247 POPS, respectively.

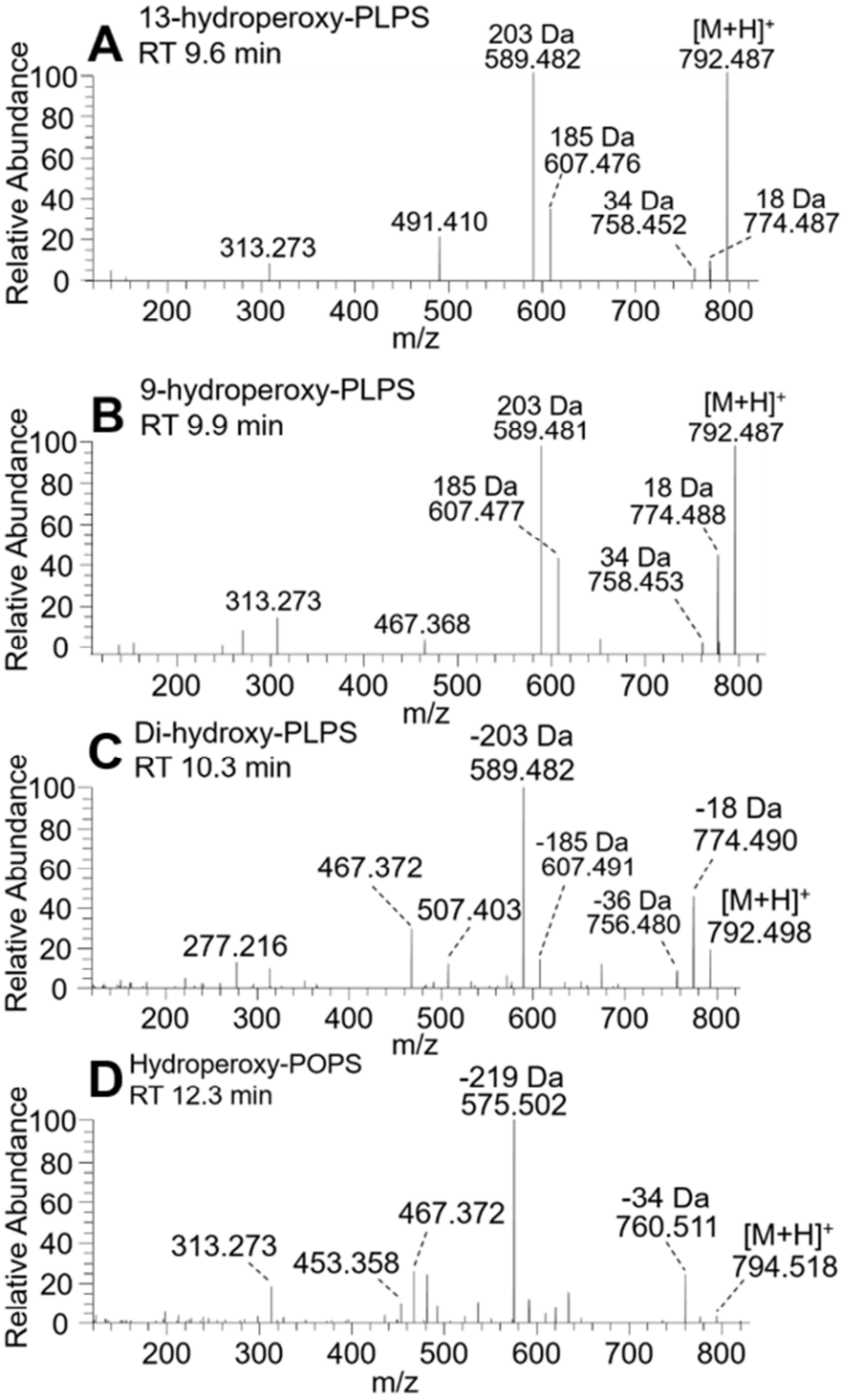

Figure 4. HCD MS/MS spectra of di-oxygenated PLPS isomers ($[M+H]^+$, *m/z* 792.501) that eluted at 9.6 min (A). 9.9 min (B) and 10.3 min (C) and di-oxygenated POPS ($[M+H]^+$ *m/z* 794.518) that eluted at 12.3 min (D).

The PLPE+2O derivatives ($[M+H]^+$, *m/z* 748.512) eluted in four peaks at RT 11.1, 11.3, 12.8 and 13.1 min (Figure 1). The discrimination of di-hydroxy-PLPE from hydroperoxy-PLPE was confirmed by the same set of product ions reported for PLPS+2O (Table 2, Supplementary Figures 5 and 6). Using the same approach, the presence of the 9-hydroperoxy positional isomer was also confirmed at RT 13.1 min (Supplementary Figure 5). The 12,15-dyhydroxy and 9,14-dihydroxy isomers were also identified at RT 11.1 min and 11.3 min (Supplementary Figure 6). All PLPE+2O and PLPS+2O species yielded a characteristic and intense product ion formed by the combined NL of water and the polar head (NL of 203 Da for PS and 159 Da for PE).

The POPE+2O derivatives eluted in one broad peak at 13.8 min (Supplementary Figure 3). The MS/MS spectrum featured the NL of H_2O, H_2O_2, and the combined NL of H_2O_2 and polar head (NL 175 Da) which confirmed the presence of hydroperoxy-POPE (Table 2, Supplementary Figure 7). The minor diagnostic product ions at *m/z* 453.357 and *m/z* 467.372 indicated the coelution of the 8-hydroperoxy and 9-hydroperoxy positional isomers, as described for hydroperoxy-POPS. Overall, the same positional isomers were found to occur for hydroperoxy-POPS and hydroperoxy-POPE and these were confirmed with a similar set of product ions.

The PLPS+3O derivatives eluted in two major peaks at RT 8.6 and 10.3 min (Supplementary Figure 1). The MS/MS spectrum acquired at 8.6 min showed the NL of polar head (185 Da), multiple NL of water molecules (18 Da and 36 Da), and combined NL of phosphoserine with 1 and 2 water molecules (203 Da and 221 Da, respectively), which overall indicated the presence of a tri-hydroxy derivative (Table 2, Figure 5A). The diagnostic product ions at *m/z* 467.372, *m/z* 505.387 and *m/z* 523.398 indicated the location of the hydroxy groups at C-9, C-12, and C-15, respectively (9,12,15-trihydroxy-PLPS isomer). The MS/MS spectrum acquired at 10.3 min showed ions arising from the combined NL of H_2O_2 and phosphoserine (219 Da) as the most abundant product ions. The NL of phosphoserine (185 Da) was also observed. The NL of H_2O_2 (34 Da), and H_2O_2 and water (52 Da) revealed that this isomer was a hydroxy-hydroperoxy-derivative;

the diagnostic product ions at *m/z* 467.372 pinpointed the hydroxy group at C-9; the diagnostic ions at *m/z* 523.399 suggested the insertion of the hydroperoxy group at C-12, whose loss of H_2O would generate the ions at *m/z* 505.387 (9-hydroxy-12-hydroperoxy-PLPS) (Figure 5B). However, the data does not exclude the formation of the isomer with the hydroxy group at C-12 and the hydroperoxy group at C-9.

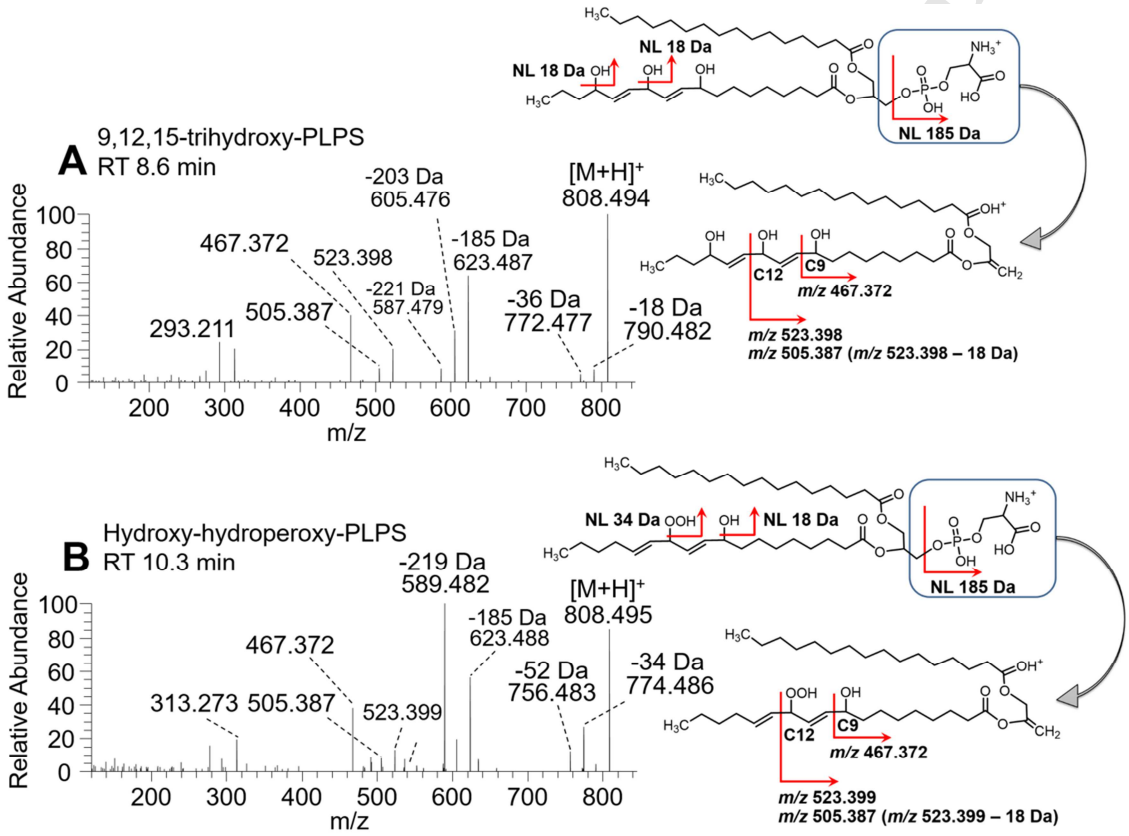

Figure 5. HCD MS/MS spectra and proposed fragmentation pathways of tri-oxygenated PLPS isomer ($[M+H]^+$, *m/z* 808.496) that eluted at 8.6 min (A) and 10.3 min (B).

PLPE+3O derivatives ($[M+H]^+$, *m/z* 764.506) eluted in two peaks at RT 9.6 and 11.2 min (Supplementary Figure 1). The first peak to elute (9.6 min) was 9,12,15-tri-hydroxy-PLPE, which MS/MS spectrum included the same set of product ions that were analysed for 9,12,15-tri-hydroxy-PLPS (Table 2, Supplementary Figure 8). The ion eluting at 11.2 min was assigned as a 9-hydroxy-12-hydroperoxy-PLPE, which also yielded the same ions described above for 9-hydroxy-12-

hydroperoxy-PLPS. The same positional isomers (9,12,15-tri-hydroxy- and 9-hydroxy-12-hydroperoxy-) were formed for both PLPE+3O and PLPS+3O.

Each of the short chain oxidation products of PE and PS eluted in one peak, as observed for 1-palmitoyl-2-oxononanoyl-PS (PONPS), 1-palmitoyl-2-azelaoyl-PS (PAzPS), 1-palmitoyl-2-oxononanoyl-PE (PONPE) and 1-palmitoyl-2-azelaoyl-PE (PAzPE), that eluted at 7.6, 7.0, 8.7 and 8.1 min, respectively (Figure 2, Supplementary Figure 1). The elution of each species in one peak suggests the presence of only one short chain derivative isomer. The MS/MS spectra of these short chain products essentially showed the NL of the polar head groups, thus hindering any additional information on the structure of the oxidatively cleaved fatty acid (Supplementary Figure 9). However, the MS/MS spectra of PONPE and PONPS showed the NL of H_2O, indicating the presence of the terminal aldehydic function.

Table 2. Summary of the most important diagnostic product ions observed in the positive ion mode HCD MS/MS spectra of oxidised PS and PE. PLPS and PLPE were chosen as an example.

	PLPS-(OH) (*m/z* 776)	**PLPS-(OOH) (*m/z* 792)**	**PLPS-$(OH)_2$ (*m/z* 792)**	**PLPS-(OH)(OOH) (*m/z* 808)**	**PLPS-$(OH)_3$ (*m/z* 808)**
NL polar head group (-185 Da)	*m/z* 591	*m/z* 607	*m/z* 607	*m/z* 623	*m/z* 623
NL H_2O (-18 Da)	*m/z* 758	*m/z* 774	*m/z* 774	*m/z* 790	*m/z* 790
NL H_2O_2 (-34 Da)		*m/z* 758		*m/z* 774	
NL *n* H_2O (*n*=2-3, -36 Da, -54 Da)			*m/z* 756		*m/z* 772
NL H_2O + H_2O_2 (-52 Da)				*m/z* 756	
NL (polar head group + H_2O) (-203 Da)	*m/z* 573	*m/z* 589	*m/z* 589	*m/z* 605	*m/z* 605
NL (polar head group + H_2O_2) (-219 Da)				*m/z* 589	
NL polar head group + Cleavage C9-C10	*m/z* 467 (C9-OH)	*m/z* 467 (C9-OOH)	*m/z* 467 (C9-OH)	*m/z* 467 (C9-OH or C9-OOH)	*m/z* 467 (C9-OH)
Cleavage C12-C13			*m/z* 674.4 (C12-OH)		
NL polar head group + Cleavage C12-C13	*m/z* 491 (C13-OH)	*m/z* 491 (C13-OOH)	*m/z* 507 (C12-OH)	*m/z* 523 (C12-OH or C12-OOH)	*m/z* 523 (C12-OH)

NL (polar head group + H_2O) + Cleavage C12-C13				*m/z* 505 (C12-OH or C12-OOH)	*m/z* 505 (C12-OH)
NL polar head group + Cleavage C13-C14					
	PLPE-(OH) (*m/z* 732)	**PLPE-(OOH) (*m/z* 748)**	**PLPE-$(OH)_2$ (*m/z* 748)**	**PLPE-(OH)(OOH) (*m/z* 764)**	**PLPE-$(OH)_3$ (*m/z* 764)**
NL polar head group (-141 Da)	*m/z* 591	*m/z* 607	*m/z* 607	*m/z* 623	*m/z* 623
NL H_2O (-18 Da)	*m/z* 714	*m/z* 730	*m/z* 730	*m/z* 746	*m/z* 746
NL H_2O_2 (-34 Da)		*m/z* 714		*m/z* 730	
NL *n* H_2O (*n*=2-3, -36 Da, -54 Da)			*m/z* 712		*m/z* 728, *m/z* 710
NL H_2O + NL H_2O_2 (-52 Da)				*m/z* 712	
NL polar head group + NL H_2O (-159 Da)	*m/z* 573	*m/z* 589	*m/z* 589	*m/z* 605	*m/z* 605
NL polar head group + NL H_2O_2 (-175 Da)		*m/z* 573		*m/z* 589	
NL polar head group + Cleavage C9-C10	*m/z* 467 (C9-OH)	*m/z* 467 (C9-OOH)	*m/z* 467 (C9-OH)	*m/z* 467 (C9-OH or C9-OOH)	*m/z* 467 (C9-OH)
Cleavage C12-C13		*m/z* 630.4	*m/z* 630.4		
NL polar head group + Cleavage C12-C13	*m/z* 491 (C13-OH)	*m/z* 507 (C12-OOH)	*m/z* 507 (C12-OH)	*m/z* 523 (C12-OH or C12-OOH)	*m/z* 523 (C12-OH)
NL (polar head group + H_2O) + Cleavage C12-C13				*m/z* 505 (C12-OH or C12-OOH)	*m/z* 505 (C12-OH)
NL polar head group + Cleavage C13-C14		*m/z* 521 (C13-OOH)			

Separation of glycoxidised derivatives of PLPE, PLPS, POPE and POPS by C30 RP-LC

The XIC of the glycoxidised derivatives of PLPE acquired in positive ion mode were plotted in Figure 6. All the glycoxidation products were found to elute earlier than non-modified PLPE, indicating that glycoxidation always led to an increased polarity of the modified APL. Glycated PLPE (*m/z* 878.576), along with the two glycoxidation products bearing an oxidatively cleaved glucose moiety on the polar head (*m/z* 744.518 and *m/z* 774.528) eluted 0.3 min, 1.1 min and 1.2 min earlier than the non-modified PLPE, respectively. Glycoxidised PLPE products with oxidation on the fatty acyl chains and an intact glucose moiety (*m/z* 894.570, *m/z* 910.565, *m/z* 770.445 and *m/z* 768.440) eluted up to 10 min earlier than the non-modified PLPE. The glycoxidised derivatives of PLPS, POPE and POPS, showed this same trend of RT (Table 1).

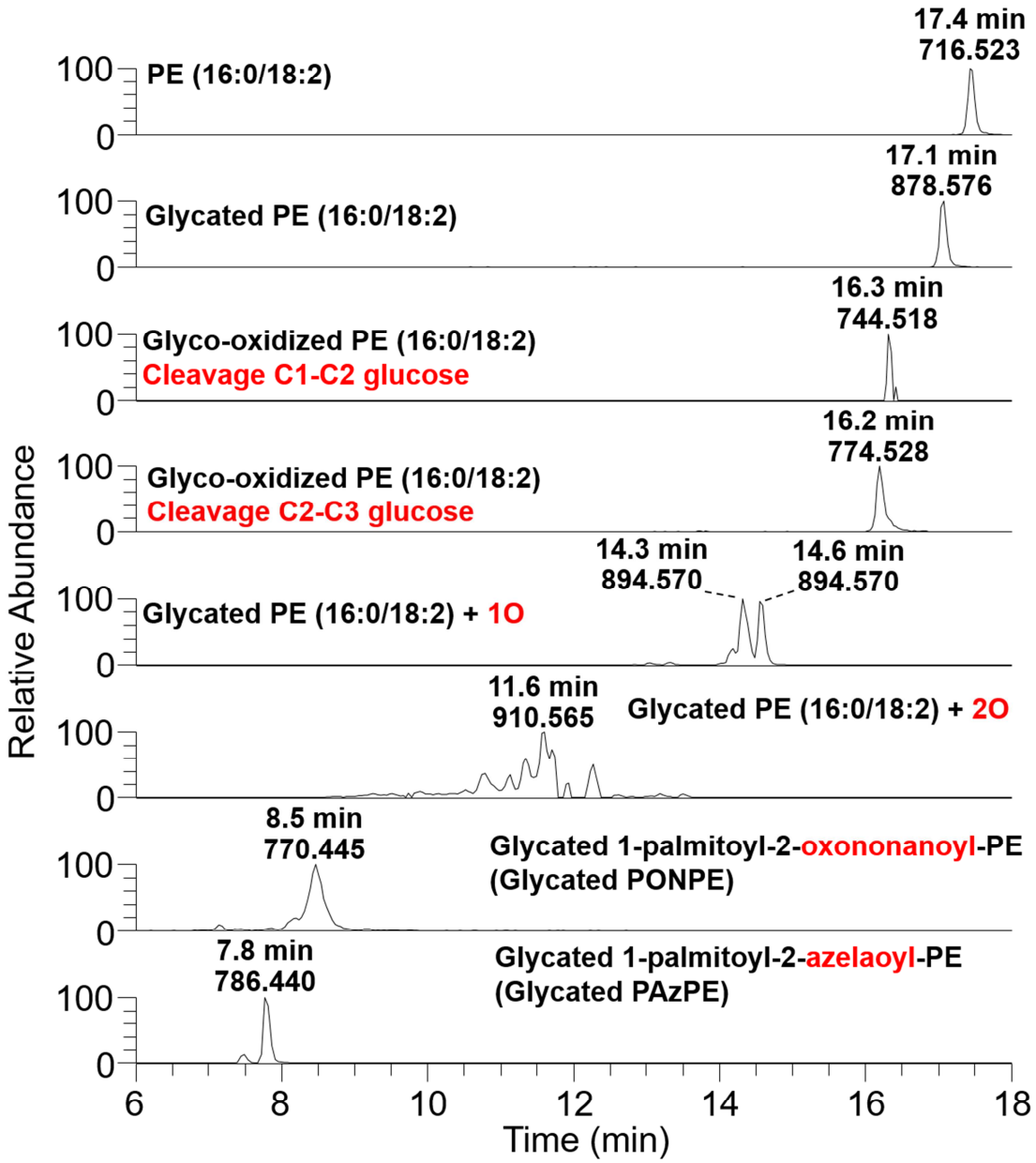

Figure 6. XIC chromatograms (±5 ppm) of PLPE and its main glycoxidation products acquired in positive ion mode.

Identification and structural characterization of glycoxidised APL with oxidation in the polar head.

Several glycoxidised derivatives of APL with oxidation in the polar head were identified, as summarised in Table 1. These glycoxidation products can be formed by the oxidative cleavage of

the glucose moiety adducted to the amino groups of APL, or by the reaction of the products derived from glucose oxidation (e.g. glyoxal or methylglyoxal) with the free polar head group of APL. In this last case, the glycoxidised derivatives are referred to as glucose-derived oxidation products. Regardless of the mechanisms involved, these final oxidation products cannot be discriminated by MS [20].

As described previously, it was not possible to identify glycoxidation occurring in the polar head for PLPS [37]. For PLPE, glycoxidised products modified in the polar head were only identified after 48 h of oxidation. Finally, glycoxidized polar head products were identifiable for POPE and POPS after 24 h Fenton oxidation (Table 1).

The MS/MS spectra acquired in positive and negative ion mode of carboxymethyl-POPE, formed by the oxidative cleavage between C-2 and C-3 of glucose, are shown in Figure 7, as an example of the fragmentation pattern of these glycoxidised APL. The only product ion observed in positive ion mode MS/MS spectrum (Figure 7A) was formed by the NL of the phosphoethanolamine polar head adducted to the carboxymethyl moiety (199 Da). The MS/MS spectrum in negative ion mode showed a NL of vinylglycine (101 Da) (Figure 7B); the carboxylate anions of the non-modified fatty acyl chains could be observed (R_1COO^- and R_2COO^-). The combined NL of vinylglycine with R_1COOH and R_2COOH was also observed at *m/z* 417.241 and *m/z* 391.226, respectively (Figure 7B) (Table 3).

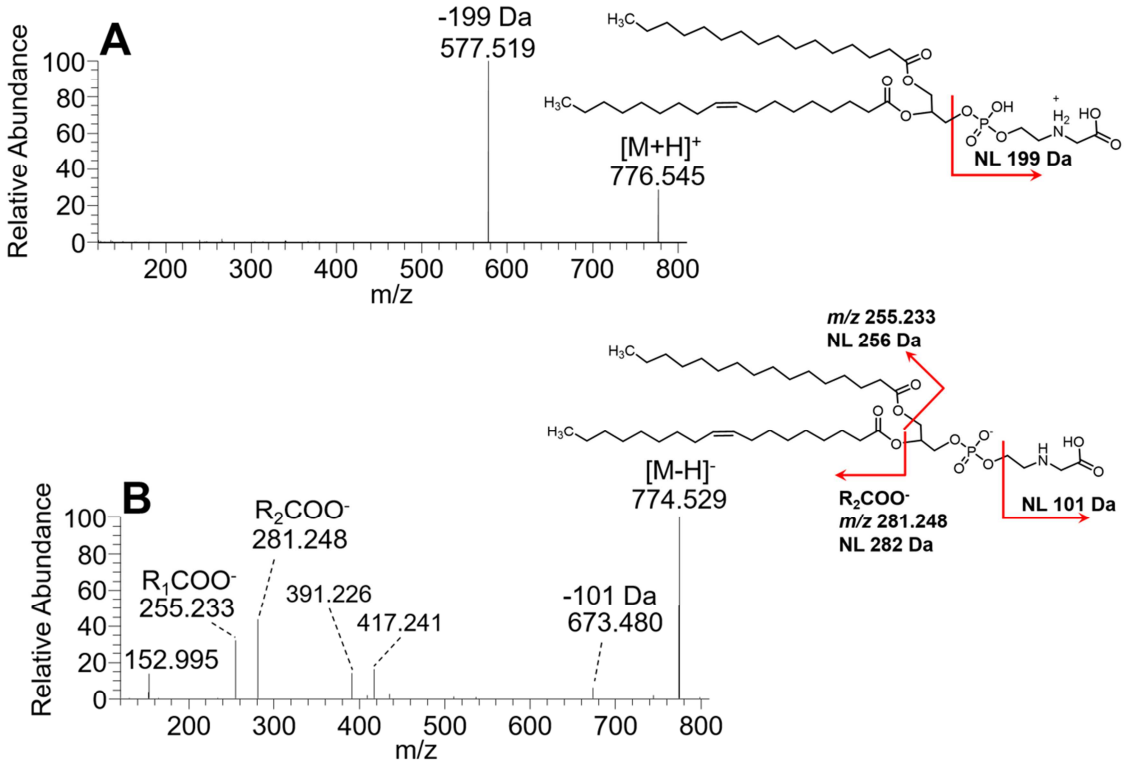

Figure 7. HCD MS/MS spectra and proposed fragmentation pathways of the glycoxidation product of POPE formed by the oxidative cleavage between C2 and C3 of glucose (carboxymethyl-POPE) that eluted at 17.2 min: $[M+H]^+$, *m/z* 776.544 (A); and $[M-H]^-$, *m/z* 774.529 (B).

Identification and structural characterisation of glycoxidised APL with oxidised fatty acyl chains.

Glycoxidized APL bearing the oxidative modification in the fatty acyl chains, but not in the polar head groups, were identified in glycated POPE, PLPE and PLPS. The glycoxidised products of POPE esterified with oxygenated fatty acyl chains could be identified only after 48 h Fenton oxidation. On the other hand, these derivatives were extensively formed during the glycoxidation of PLPE. Glycoxidized derivatives of POPS were not observed, while glycoxidation of PLPS exclusively led to the formation of glycated PAzPS (Table 1). The positive ion mode MS/MS spectrum of glycated PAzPS, acquired at RT 6.2 min, showed the NL of glycated

phosphoethanolamine polar head (303 Da) and NL of water. In negative ion mode, the MS/MS spectra showed the carboxylate anions arising from palmitic acid (R_1COO^-) and azelaic acid (R_2'COO^-), along with products ions arising from the NL of glucose (162 Da), and the NL of $C_4H_8O_4$ (120 Da) (Table 3) [46,47].

Glycoxidised PLPE with one hydroxy group on linoleic acid ($[M+H]^+$, *m/z* 894.571) eluted in two peaks at RT 14.3 and 14.6 min (Figure 6). The MS/MS spectrum of the derivative at 14.6 min (Figure 8A) showed four NL of water molecules. Three of these NL were due to the fragmentation of the non-modified glucose moiety [46,47], and the other NL of water was therefore due to the presence of the hydroxy moiety on the fatty acyl chain. The NL of glycated phosphoethanolamine (303 Da), and glycated phosphoethanolamine plus H_2O (321 Da) were also observed. The product ions at *m/z* 467.371 located the hydroxy group at C-9 of the linoleoyl chain, as reported for hydroxy-PLPE. The MS/MS spectrum of the glycoxidised PLPE derivative at 14.3 min (Figure 8B) showed the same product ions described above for the other isomer, but the presence of the ion at *m/z* 491.409 located the hydroxy group at C-13 (Table 3).

A glycoxidised derivative with di-oxygenated fatty acyl chain was identified exclusively for PLPE, glycoxidised PLPE+2O ($[M+H]^+$, *m/z* 910.566), which eluted in several peaks between RT 10 and 12.5 min (Figure 6). The MS/MS spectrum at 11.1 min (Figure 8C) showed two NL of water (18 Da, 36 Da), one combined NL of H_2CO and water (84 Da) and a NL of the glycated polar head (303 Da). The product ion formed by the combined loss of the glycated polar head and water (321 Da) was the base peak. Altogether, the fragmentation pattern of glycoxidised PLPE+2O was very similar to the one reported above for PLPE+2O (Supplementary Figures 5 and 6). The presence of the consecutive NL of water suggested the formation of a glycoxidised PLPE with two hydroxy groups on the linoleic acid chain. The absence of a NL of H_2O_2 (34 Da) excluded the presence of a hydroperoxy group. The product ions at *m/z* 467.374 located the first hydroxy group at C9, indicating the formation of the 9,14-dihydroxy-isomer. The MS/MS spectrum of glycoxidised

PLPE+2O at 11.6 minutes showed essentially the same product ions as described earlier. However, the presence of the product ions at *m/z* 507.405 suggested the formation of the 12,15-dihydroxy-isomer (Figure 8D). The same isomers (9,14-dihydroxy and 12,15-dihydroxy) were observed for di-hydroxy-PLPE (Supplementary Figure 6) and di-hydroxy-PLPS (Figure 4) (Table 3).

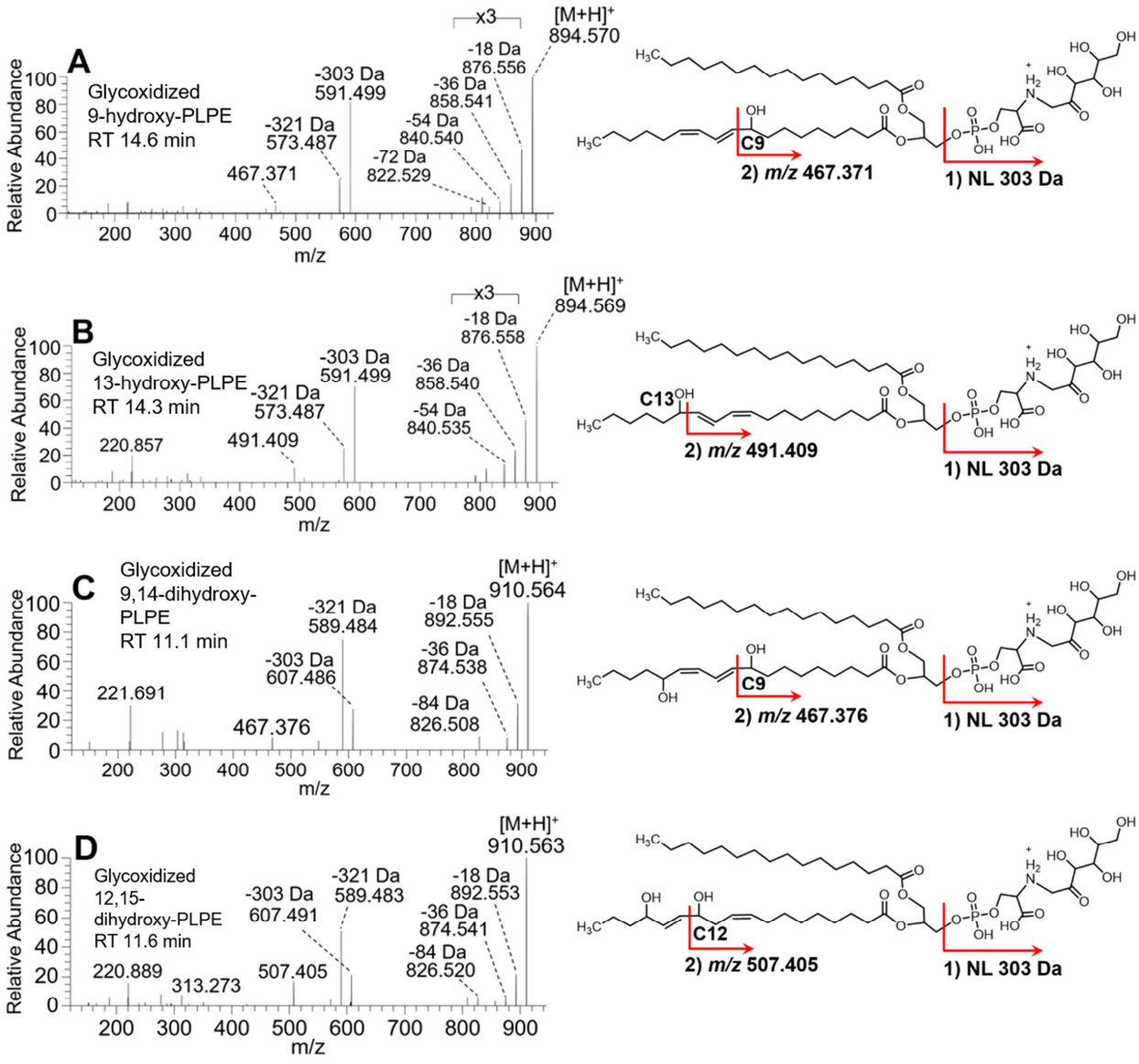

Figure 8. HCD MS/MS spectra and proposed fragmentation pathways of glycoxidised PLPE + 1O isomers ($[M+H]^+$, *m/z* 894.570) that eluted at 14.6 min (A) and 14.3 min (B) and of the glycoxidised PLPE + 2O isomers ($[M+H]^+$, *m/z* 910.565) that eluted at 11.1 min (C) and 11.6 min (D).

Table 3. Summary of the most important diagnostic product ions observed in the positive ion mode HCD MS/MS spectra of glycoxidised PLPE.

	Glycated PLPE	**Formyl-PLPE (Glucose cleavage C1-C2)**	**Carboxymethyl-PLPE (Glucose cleavage C2-C3)**	**Glycated PLPE-(OH)**	**Glycated PLPE-(OH-OH)**
NL modified polar head group	*m/z* 575	*m/z* 575	*m/z* 575	*m/z* 591	*m/z* 607
NL H_2O (-18 Da)	*m/z* 860			*m/z* 876	*m/z* 892
NL nH_2O (*n*=2-3, -36 Da, -54 Da)				*m/z* 858, *m/z* 840	*m/z* 874, *m/z* 858
(1) NL modified polar head group (2) NL H_2O				*m/z* 573	*m/z* 589
(1) NL modified polar head group (2) Cleavage C9-C10				*m/z* 467 (C9-OH)	*m/z* 467 (C9-OH)
(1) NL modified polar head group (2) Cleavage C12-C13				*m/z* 491 (C13-OH)	*m/z* 507 (C12-OH)

Discussion

In the present work, C30 RP-LC-MS and HCD MS/MS were used for the first time to separate and identify the structural and functional group isomers of oxidised and glycoxidised APL. The structural identification was based on the exact mass measurements, RT, and specific fragment ions formed under HCD MS/MS. The retention of modified lipids on the C30 column changed clearly with the type of modification, and in some cases with the location of the modifications along the fatty acyl chain. Long chain oxidation products of APL eluted earlier than non-modified APL, and short chain oxidation products eluted even earlier than long chain products. These observations were in accordance with previous studies on RP-LC of oxidised PE [32] and PS [37]. As expected, the insertion of more than one oxygen progressively weakened the interaction of the oxidation product with the C30 column. Several oxygenated derivatives (APL+ nO, n= 1-3), were also

406 identified for APL including the APL bearing linoleic acid. It is known that oleic acid is much less
407 prone to radical oxidation than linoleic acid and other polyunsaturated fatty acids because it lacks
408 bis-allylic carbons. However, oleic acid has two allylic positions that can react with radicals such as
409 •OH, and oxidation products of oleic acid esterified in PC [48], PE [45] and PS [20] were identified
410 previously. In the case of linoleic acid esterified to phospholipids, the presence of both bis-allylic
411 and allylic positions allows the abstraction of hydrogens from more than one carbon, and thus the
412 oxidation in different positions in the same fatty acyl chain. Poly-oxygenated APL esterified to
413 linoleic acid were already reported *in vitro* [32] and in apoptotic cells [9].

414 The separation of functional isomers was achieved in this work, with hydroxy derivatives
415 eluting earlier than hydroperoxy APL. Previously, Domingues et al. [32] attained the separation of
416 hydroperoxy-PLPE and di-hydroxy-PLPE on C5 LC-MS/MS. Later, C5 RP-LC was again proposed
417 for the chromatographic separation of two isobaric short chain oxidation products of PS, namely a
418 gamma-hydroperoxy aldehyde and a gamma-hydroxy carboxylic acid [37]. Also, the present C30
419 LC method attained the separation of positional isomers of several oxidised APL, for example, 9-
420 hydroxy-PLPS and 13-hydroxy-PLPS, or 9,14-dihydroxy-PLPE and 12,15-dihydroxy-PLPE. A
421 similar result has never been achieved during the analysis of oxidised APL with C5 columns, but
422 one study reported the separation of six positional isomers of hydroxy-SAPE using a C18 column
423 [49].

424 For glycoxidised APL, the oxidative cleavages occurring in the glycated polar head slightly
425 increased the polarity of the derivatives, which eluted approximately 1 minute earlier than the
426 correspondent non-modified APL. When the oxidation affected the fatty acyl chain, the
427 glycoxidised derivatives eluted up to 10 minutes earlier than the non-modified APL. Glycoxidised
428 APL with a truncated fatty acyl chain were the most polar derivatives, eluting with the lowest RT.
429 Other studies with C5 LC-MS analysis of both glycoxidised PE [33] and PS [37] observed a similar
430 trend. In these studies, all the derivatives modified in the fatty acyl chains eluted at lowest RT when

compared with the derivatives modified at the glucose moiety or in the polar head. However, neither of these studies succeeded to resolve positional isomers. Notably, the C30 column achieved the separation of positional isomers of glycoxidised PLPE bearing oxidative modifications at distinct positions of the fatty acyl chain.

In this work, specific HCD-MS/MS fragmentation patterns were identified for modified APL, as summarised in Figure 9, that illustrated all the fragmentation pathways observed for oxidised and glycoxidised PE and PS. The NL of water and H_2O_2 discriminated functional isomers as poly-hydroxy-APL and hydroperoxy-APL, as already reported in other studies carried out using CID as fragmentation method [32,45,48]. Fragments arising from the NL of water and polar heads (159 Da and 203 Da for PE and PS, respectively) were MS/MS signatures characterising all hydroxy derivatives. For these molecules, the NL of the polar head (141 Da and 185 Da for PE and PS, respectively) originated the most abundant fragment ions, as already observed in previous reports that used CID [5,44]. However, in the case of di-hydroxy and hydroperoxy derivatives, the base peak in the MS/MS spectra arose from the combined NL of water and polar heads (159 Da and 203 Da for PE and PS, respectively), which appear to be intense MS/MS signatures of all di-oxygenated derivatives of APL. Finally, the combined NL of H_2O_2 and polar head (175 Da and 219 Da for PE and PS, respectively) were the most abundant MS/MS fragments in all hydroxy-hydroperoxy APL. The assignment of the position of the oxygenated moieties defining positional isomers was always achieved using the information from the positive ion mode fragmentation between the oxygenated carbon and the carbon involved in the double bond in a vinylic position [23,32].

Glycoxidized APL with an oxidatively cleaved glucose moiety showed specific positive ion mode HCD MS/MS fragment ions, formed by the NL of the modified polar head [33,35]. Glycated PE and glycoxidised PE modified only at the fatty acyl chains showed positive ion mode MS/MS characteristic fragment ions arising from the NL of glycated phosphoethanolamine (303 Da), along

456 with several NL of water [21,33]. The fragmentation patterns that allowed the assignment of the
457 position of the functional group along the fatty acyl chain were the same in oxidised and
458 glycoxidised APL (Tables 2 and 3).

459

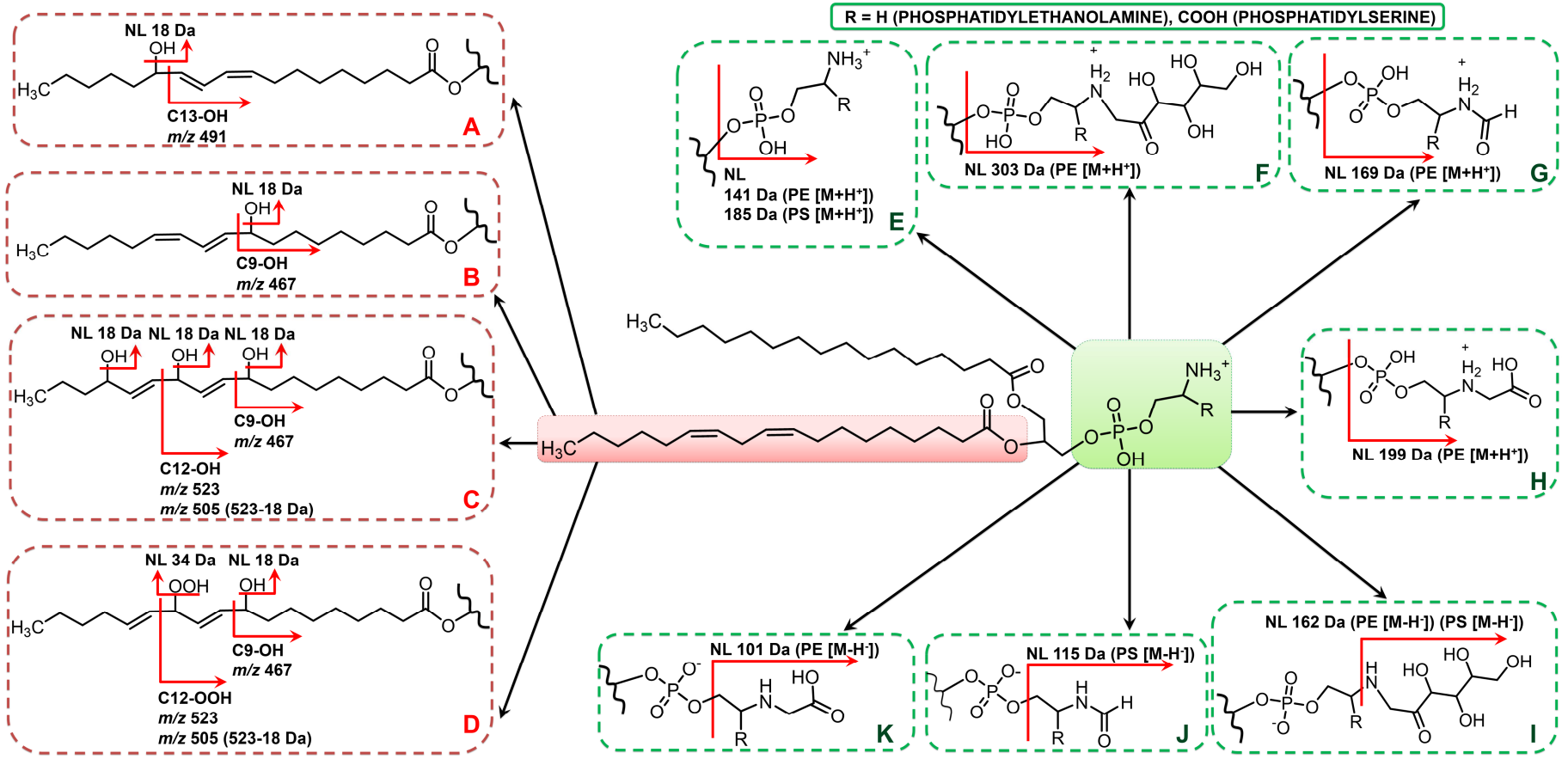

Figure 9. A comprehensive overview of all the fragmentation pathways observed and described in the present work for oxidised and glycoxidised PE and PS. The fragmentation pathways of the oxidative modifications occurring on the unsaturated sn-2 fatty acyl chain (shaded red box) are summarised into dashed red boxes (A-D). The fragmentation pathways of the glycoxidative modifications occurring on the polar head (shaded green box) are summarised into dashed green boxes (E-K). A, NL of H_2O and fragmentation of the C12-C13 bond (occurs in positive ion

mode for 13-hydroxy-PLPE and PLPS after the NL of the polar head). B, NL of H_2O and fragmentation of the C9-C10 bond (occurs in positive ion mode for 9-hydroxy-PLPE and PLPS after the NL of the polar head). C, multiple NL of H_2O and fragmentation of the C9-C10 and C12-C13 bonds (occurs in positive ion mode for 9,12,15-trihydroxy-PLPE and PLPS after the NL of the polar head). D, NL of H_2O and H_2O_2 and fragmentation of the C9-C10 and C12-C13 bonds (occurs in positive ion mode for 9-hydroxy-12-hydroperoxy PLPE and PLPS, and 12-hydroxy-9-hydroperoxy-PLPE and PLPS, after the NL of the polar head). E, NL of the phosphoethanolamine and phosphoserine polar heads (occurs in positive ion mode for PE and PS species, respectively). F, NL of the glycated polar head (occurs in positive ion mode for glycated PE species and glycoxidised PE species with oxidative modifications on the fatty acyl chains). G, NL of modified polar head (occurs in positive ion mode for glycoxidised PE after the oxidative cleavage of the glucose moiety) (C1-C2). H, NL of modified polar head (occurs in positive ion mode for glycoxidised PE after oxidative cleavage of the glucose moiety) (C2-C3). I, NL of glucose (occurs in negative ion mode for glycated PE and PS and glycoxidised PE and PS species with oxidative modifications on the fatty acyl chains). J, NL of 2-formamidoacrylic acid (occurs in negative ion mode for glycoxidised PS after the oxidative cleavage of the glucose moiety) (C1-C2). K, NL of vinylglycine (occurs in negative ion mode for glycoxidised PE after the cleavage of the glucose moiety) (C2-C3).

The potential of C30 LC-MS and MS/MS for the separation and identification of isomers of modified APL can be further explored to screen for these low abundant lipids in complex biological samples. Some of the oxidation products identified herein were already detected *in vivo* and reported to have many specific biological roles. Different positional isomers of oxidized PE (5-hydroxy, 12-hydroxy and 15-hydroxy) formed by lipoxygenase (LOX) were detected by LC-MS/MS in activated monocytes/macrophages [14–16,50,51], neutrophils [50–52] and platelets [15,50,51,53,54] and were correlated with blood coagulation [54], modulation of inflammation [14], and ferroptosis [7], suggesting a structure-activity relationship. Radical-driven oxidation of APL was also reported to occur in the retina from rats [31], lung from mice exposed to γ radiation [43], and brain from humans with Alzheimer's disease [17]. Also, radical oxidised PE and PS were associated with apoptotic cell death [9,55] and with several functions resulting in a multifaceted modulation of the immune system [11–13,56,57].

Conclusions.

Oxidised and glycoxidised PE and PS represent a group of molecules which biological relevance has been increasingly reported over the last years. However, their analysis still faces several difficulties, such as the large structural complexity of isomers of modified APL, and their low relative abundance *in vivo*. In this work, an LC-MS/MS analytical platform comprised of C30 RP-LC, high-resolution MS, and HCD MS/MS, suitable for lipidomic studies, was applied for the analysis of oxidised and glycoxidised APL. This LC platform accomplished the separation of non-modified APL from oxidised and glycoxidised APL, along with with the separation of functional isomers, and the discrimination of positional isomers of modified APL, solving the issue of co-eluting species that affected many other previously tested RP-LC protocols. Fragmentations involving the NL of water and H_2O_2 were MS/MS signatures that confirmed functional group isomers of oxidised and glycoxidised APL. Specific fragmentations occurring along the oxidised fatty acyl chains were indicators of the position of the functional

group. Overall, the results gathered herein are important in the lipidomic analyses of biological samples and in the development of new targeted LC-MS/MS methods that can perform highly accurate, selective and sensitive analysis of oxidised and glycoxidised APL in biological and clinical samples.

Acknowledgements.

Thanks are due to University of Aveiro, Thermo Fisher Scientific Bremen, European Commission's Horizon 2020 research and innovation programme under the Marie Sklodowska-Curie grant agreement number 675132 (MSCA-ITN-ETN MASSTRPLAN), Marine Lipidomics Laboratory, Fundação para a Ciência e a Tecnologia (FCT, MECPortugal), European Union, QREN, Programa Operacional Factores de Competitividade (COMPETE) and FEDER for the financial support to QOPNA research Unit (FCT UID/QUI/00062/2019), to CESAM (UID/AMB/50017/2019), to Portuguese Mass Spectrometry Network (LISBOA-01-0145-FEDER-402-022125), FCT/MEC through national funds, and the co-funding by the FEDER, within the PT2020 Partnership Agreement and Compete 2020. Financial support from the German Federal Ministry of Education and Research (BMBF) within the framework of the e:Med research and funding concept for SysMedOS project (to MF) are gratefully acknowledged.

Declarations of interest.

None.

List of abbreviations.

$^{\bullet}$OH	Hydroxyl radical
APL	Aminophospholipid

AU	Arbitrary units
H_2O	Water
H_2O_2	Hydrogen peroxide
HCD	Higher-energy C-trap dissociation
LC-MS/MS	Liquid chromatography-tandem mass spectrometry
NL	Neutral loss
PAzPE	1-palmitoyl-2-azelaoyl-PE
PAzPS	1-palmitoyl-2-azelaoyl-PS
PC	Phosphatidylcholine
PE	Phosphatidylethanolamine
PLPE	1-palmitoyl-2-linoleoyl-sn-3-glycerophosphoethanolamine
PLPS	1-palmitoyl-2-linoleoyl-sn-3-glycerophosphoserine
PONPE	1-palmitoyl-2-oxononanoyl-PE
PONPS	1-palmitoyl-2-oxononanoyl-PS
POPE	1-palmitoyl-2-oleoyl-sn-3-glycerophosphoethanolamine
POPS	1-palmitoyl-2-oleoyl-sn-3-glycerophosphoserine
PS	Phosphatidylserine
ROS	Reactive oxygen species

RP	Reversed phase
RT	Retention time
SAPE	1-stearoyl-2-arachidonoyl-sn-3-glycerophosphoethanolamine
XIC	Extracted ion current

References.

[1] J.E. Vance, G. Tasseva, Formation and function of phosphatidylserine and phosphatidylethanolamine in mammalian cells, Biochim. Biophys. Acta BBA - Mol. Cell Biol. Lipids. 1831 (2013) 543–554. doi:10.1016/j.bbalip.2012.08.016.

[2] G.O. Fruhwirth, A. Loidl, A. Hermetter, Oxidized phospholipids: From molecular properties to disease, Biochim. Biophys. Acta BBA - Mol. Basis Dis. 1772 (2007) 718–736. doi:10.1016/j.bbadis.2007.04.009.

[3] V.N. Bochkov, O.V. Oskolkova, K.G. Birukov, A.-L. Levonen, C.J. Binder, J. Stöckl, Generation and biological activities of oxidized phospholipids, Antioxid. Redox Signal. 12 (2010) 1009–1059.

[4] M.R.M. Domingues, A. Reis, P. Domingues, Mass spectrometry analysis of oxidized phospholipids, Chem. Phys. Lipids. 156 (2008) 1–12. doi:10.1016/j.chemphyslip.2008.07.003.

[5] V.B. O'Donnell, Mass spectrometry analysis of oxidized phosphatidylcholine and phosphatidylethanolamine, Biochim. Biophys. Acta BBA - Mol. Cell Biol. Lipids. 1811 (2011) 818–826. doi:10.1016/j.bbalip.2011.07.018.

[6] A. Reis, C.M. Spickett, Chemistry of phospholipid oxidation, Biochim. Biophys. Acta BBA - Biomembr. 1818 (2012) 2374–2387. doi:10.1016/j.bbamem.2012.02.002.

[7] V.E. Kagan, G. Mao, F. Qu, J.P.F. Angeli, S. Doll, C.S. Croix, H.H. Dar, B. Liu, V.A. Tyurin, V.B. Ritov, A.A. Kapralov, A.A. Amoscato, J. Jiang, T. Anthonymuthu, D. Mohammadyani, Q. Yang, B. Proneth, J. Klein-Seetharaman, S. Watkins, I. Bahar, J. Greenberger, R.K. Mallampalli, B.R. Stockwell, Y.Y. Tyurina, M. Conrad, H. Bayır, Oxidized arachidonic and adrenic PEs navigate cells to ferroptosis, Nat. Chem. Biol. 13 (2016) 81–90. doi:10.1038/nchembio.2238.

[8] M.E. Greenberg, M. Sun, R. Zhang, M. Febbraio, R. Silverstein, S.L. Hazen, Oxidized phosphatidylserine–CD36 interactions play an essential role in macrophage-dependent phagocytosis of apoptotic cells, J. Exp. Med. 203 (2006) 2613–2625. doi:10.1084/jem.20060370.

[9] V.A. Tyurin, K. Balasubramanian, D. Winnica, Y.Y. Tyurina, A.S. Vikulina, R.R. He, A.A. Kapralov, C.H. Macphee, V.E. Kagan, Oxidatively modified phosphatidylserines on the surface of apoptotic cells are essential phagocytic "eat-me" signals: cleavage and inhibition of phagocytosis by Lp-PLA2, Cell Death Differ. 21 (2014) 825–835. doi:10.1038/cdd.2014.1.

[10] C. Simões, A.C. Silva, P. Domingues, P. Laranjeira, A. Paiva, M.R.M. Domingues, Modified phosphatidylethanolamines induce different levels of cytokine expression in monocytes and dendritic cells, Chem. Phys. Lipids. 175–176 (2013) 57–64. doi:10.1016/j.chemphyslip.2013.07.008.

[11] S. Colombo, C. Martín-Sierra, T. Melo, P. Laranjeira, A. Paiva, P. Domingues, M.R. Domingues, Modulation of the inflammatory response of immune cells in human peripheral

blood by oxidized arachidonoyl aminophospholipids, Arch. Biochem. Biophys. 660 (2018) 64–71. doi:10.1016/j.abb.2018.10.003.

[12] R.N. da Silva, A.C. Silva, E. Maciel, C. Simões, S. Horta, P. Laranjeira, A. Paiva, P. Domingues, M.R.M. Domingues, Evaluation of the capacity of oxidized phosphatidylserines to induce the expression of cytokines in monocytes and dendritic cells, Arch. Biochem. Biophys. 525 (2012) 9–15. doi:10.1016/j.abb.2012.05.022.

[13] E. von Schlieffen, O.V. Oskolkova, G. Schabbauer, F. Gruber, S. Bluml, M. Genest, A. Kadl, C. Marsik, S. Knapp, J. Chow, N. Leitinger, B.R. Binder, V.N. Bochkov, Multi-Hit Inhibition of Circulating and Cell-Associated Components of the Toll-Like Receptor 4 Pathway by Oxidized Phospholipids, Arterioscler. Thromb. Vasc. Biol. 29 (2009) 356–362. doi:10.1161/ATVBAHA.108.173799.

[14] V.J. Hammond, A.H. Morgan, S. Lauder, C.P. Thomas, S. Brown, B.A. Freeman, C.M. Lloyd, J. Davies, A. Bush, A.-L. Levonen, E. Kansanen, L. Villacorta, Y.E. Chen, N. Porter, Y.M. Garcia-Diaz, F.J. Schopfer, V.B. O'Donnell, Novel Keto-phospholipids Are Generated by Monocytes and Macrophages, Detected in Cystic Fibrosis, and Activate Peroxisome Proliferator-activated Receptor-, J. Biol. Chem. 287 (2012) 41651–41666. doi:10.1074/jbc.M112.405407.

[15] B.H. Maskrey, A. Bermudez-Fajardo, A.H. Morgan, E. Stewart-Jones, V. Dioszeghy, G.W. Taylor, P.R.S. Baker, B. Coles, M.J. Coffey, H. Kuhn, V.B. O'Donnell, Activated Platelets and Monocytes Generate Four Hydroxyphosphatidylethanolamines via Lipoxygenase, J. Biol. Chem. 282 (2007) 20151–20163. doi:10.1074/jbc.M611776200.

[16] A.H. Morgan, V. Dioszeghy, B.H. Maskrey, C.P. Thomas, S.R. Clark, S.A. Mathie, C.M. Lloyd, H. Kuhn, N. Topley, B.C. Coles, P.R. Taylor, S.A. Jones, V.B. O'Donnell, Phosphatidylethanolamine-esterified Eicosanoids in the Mouse: TISSUE LOCALIZATION AND INFLAMMATION-DEPENDENT FORMATION IN Th-2 DISEASE, J. Biol. Chem. 284 (2009) 21185–21191. doi:10.1074/jbc.M109.021634.

[17] R.A. Maki, V.A. Tyurin, R.C. Lyon, R.L. Hamilton, S.T. DeKosky, V.E. Kagan, W.F. Reynolds, Aberrant Expression of Myeloperoxidase in Astrocytes Promotes Phospholipid Oxidation and Memory Deficits in a Mouse Model of Alzheimer Disease, J. Biol. Chem. 284 (2009) 3158–3169. doi:10.1074/jbc.M807731200.

[18] E. Maciel, B.M. Neves, D. Santinha, A. Reis, P. Domingues, M. Teresa Cruz, A.R. Pitt, C.M. Spickett, M.R.M. Domingues, Detection of phosphatidylserine with a modified polar head group in human keratinocytes exposed to the radical generator AAPH, Arch. Biochem. Biophys. 548 (2014) 38–45. doi:10.1016/j.abb.2014.02.002.

[19] A. Ravandi, A. Kuksis, L. Marai, J.J. Myher, G. Steiner, G. Lewisa, H. Kamido, Isolation and identification of glycated aminophospholipids from red cells and plasma of diabetic blood, FEBS Lett. 381 (1996) 77–81.

[20] E. Maciel, R.N. da Silva, C. Simões, T. Melo, R. Ferreira, P. Domingues, M.R.M. Domingues, Liquid chromatography–tandem mass spectrometry of phosphatidylserine advanced glycated end products, Chem. Phys. Lipids. 174 (2013) 1–7. doi:10.1016/j.chemphyslip.2013.05.005.

[21] A. Annibal, T. Riemer, O. Jovanovic, D. Westphal, E. Griesser, E.E. Pohl, J. Schiller, R. Hoffmann, M. Fedorova, Structural, biological and biophysical properties of glycated and glycoxidised phosphatidylethanolamines, Free Radic. Biol. Med. 95 (2016) 293–307. doi:10.1016/j.freeradbiomed.2016.03.011.

[22] K. Nakagawa, Ion-trap tandem mass spectrometric analysis of Amadori-glycated phosphatidylethanolamine in human plasma with or without diabetes, J. Lipid Res. 46 (2005) 2514–2524. doi:10.1194/jlr.D500025-JLR200.

[23] C. Simões, A.C. Silva, P. Domingues, P. Laranjeira, A. Paiva, M.R.M. Domingues, Phosphatidylethanolamines Glycation, Oxidation, and Glycoxidation: Effects on Monocyte and Dendritic Cell Stimulation, Cell Biochem. Biophys. 66 (2013) 477–487. doi:10.1007/s12013-012-9495-2.

[24] J.R. Requena, M.U. Ahmed, C.W. Fountain, T.P. Degenhardt, S. Reddy, C. Perez, T.J. Lyons, A.J. Jenkins, J.W. Baynes, S.R. Thorpe, Carboxymethylethanolamine, a biomarker of phospholipid modification during the maillard reaction in vivo, J. Biol. Chem. 272 (1997) 17473–17479.
[25] W.C. Fountain, J.R. Requena, A.J. Jenkins, T.J. Lyons, B. Smyth, J.W. Baynes, S.R. Thorpe, Quantification of N-(Glucitol)ethanolamine and N-(Carboxymethyl)serine: Two Products of Nonenzymatic Modification of Aminophospholipids Formed in Vivo, Anal. Biochem. 272 (1999) 48–55. doi:10.1006/abio.1999.4147.
[26] S. Lertsiri, M. Shiraishi, T. Miyazawa, Identification of Deoxy-Fructosyl Phosphatidylethanolamine as a Non-enzymic Glycation Product of Phosphatidylethanolamine and its Occurrence in Human Blood Plasma and Red Blood Cells, Biosci. Biotechnol. Biochem. 62 (1998) 893–901. doi:10.1271/bbb.62.893.
[27] C.M. Breitling-Utzmann, A. Unger, D.A. Friedl, M.O. Lederer, Identification and Quantification of Phosphatidylethanolamine- Derived Glucosylamines and Aminoketoses from Human ErythrocytesÐInfluence of Glycation Products on Lipid Peroxidation, Arch. Biochem. Biophys. 391 (2001) 245–254. doi:10.1006/abbi.2001.2406.
[28] N. Shoji, K. Nakagawa, A. Asai, I. Fujita, A. Hashiura, Y. Nakajima, S. Oikawa, T. Miyazawa, LC-MS/MS analysis of carboxymethylated and carboxyethylated phosphatidylethanolamines in human erythrocytes and blood plasma, J. Lipid Res. 51 (2010) 2445–2453. doi:10.1194/jlr.D004564.
[29] P. Sookwong, K. Nakagawa, I. Fujita, N. Shoji, T. Miyazawa, Amadori-Glycated Phosphatidylethanolamine, a Potential Marker for Hyperglycemia, in Streptozotocin-Induced Diabetic Rats, Lipids. 46 (2011) 943–952. doi:10.1007/s11745-011-3588-3.
[30] R. Pamplona, J.R. Requena, M. Portero-Otín, J. Prat, S.R. Thorpe, M.J. Bellmunt, Carboxymethylated phosphatidylethanolamine in mitochondrial membranes of mammals, Eur. J. Biochem. 255 (1998) 685–689.
[31] B.G. Gugiu, C.A. Mesaros, M. Sun, X. Gu, J.W. Crabb, R.G. Salomon, Identification of Oxidatively Truncated Ethanolamine Phospholipids in Retina and Their Generation from Polyunsaturated Phosphatidylethanolamines, Chem. Res. Toxicol. 19 (2006) 262–271. doi:10.1021/tx050247f.
[32] M.R.M. Domingues, C. Simões, J.P. da Costa, A. Reis, P. Domingues, Identification of 1-palmitoyl-2-linoleoyl-phosphatidylethanolamine modifications under oxidative stress conditions by LC-MS/MS, Biomed. Chromatogr. 23 (2009) 588–601. doi:10.1002/bmc.1157.
[33] C. Simões, V. Simões, A. Reis, P. Domingues, M.R.M. Domingues, Oxidation of glycated phosphatidylethanolamines: evidence of oxidation in glycated polar head identified by LC-MS/MS, Anal. Bioanal. Chem. 397 (2010) 2417–2427. doi:10.1007/s00216-010-3825-2.
[34] T. Melo, N. Santos, D. Lopes, E. Alves, E. Maciel, M.A.F. Faustino, J.P.C. Tomé, M.G.P.M.S. Neves, A. Almeida, P. Domingues, M.A. Segundo, M.R.M. Domingues, Photosensitized oxidation of phosphatidylethanolamines monitored by electrospray tandem mass spectrometry: ESI-MS of photosensitized phosphatidylethanolamines, J. Mass Spectrom. 48 (2013) 1357–1365. doi:10.1002/jms.3301.
[35] T. Melo, E.M.P. Silva, C. Simões, P. Domingues, M.R.M. Domingues, Photooxidation of glycated and non-glycated phosphatidylethanolamines monitored by mass spectrometry: Photooxidation of PE and GlucPE, J. Mass Spectrom. 48 (2013) 68–78. doi:10.1002/jms.3129.
[36] E. Maciel, R.N. da Silva, C. Simões, P. Domingues, M.R.M. Domingues, Structural Characterization of Oxidized Glycerophosphatidylserine: Evidence of Polar Head Oxidation, J. Am. Soc. Mass Spectrom. 22 (2011) 1804–1814. doi:10.1007/s13361-011-0194-9.
[37] E. Maciel, R. Faria, D. Santinha, M.R.M. Domingues, P. Domingues, Evaluation of oxidation and glyco-oxidation of 1-palmitoyl-2-arachidonoyl-phosphatidylserine by LC–MS/MS, J. Chromatogr. B. 929 (2013) 76–83. doi:10.1016/j.jchromb.2013.04.009.

[38] K. Zemski Berry, W. Turner, M. VanNieuwenhze, R. Murphy, Characterization of oxidized phosphatidylethanolamine derived from RAW 264.7 cells using 4-(dimethylamino)benzoic acid derivatives, Eur. J. Mass Spectrom. 16 (2010) 463. doi:10.1255/ejms.1083.
[39] T. Houjou, K. Yamatani, M. Imagawa, T. Shimizu, R. Taguchi, A shotgun tandem mass spectrometric analysis of phospholipids with normal-phase and/or reverse-phase liquid chromatography/electrospray ionization mass spectrometry, Rapid Commun. Mass Spectrom. 19 (2005) 654–666. doi:10.1002/rcm.1836.
[40] E. Rampler, A. Criscuolo, M. Zeller, Y. El Abiead, H. Schoeny, G. Hermann, E. Sokol, K. Cook, D.A. Peake, B. Delanghe, G. Koellensperger, A Novel Lipidomics Workflow for Improved Human Plasma Identification and Quantification Using RPLC-MSn Methods and Isotope Dilution Strategies, Anal. Chem. 90 (2018) 6494–6501. doi:10.1021/acs.analchem.7b05382.
[41] M. Narváez-Rivas, Q. Zhang, Comprehensive untargeted lipidomic analysis using core-shell C30 particle column and high field orbitrap mass spectrometer, J. Chromatogr. A. 1440 (2016) 123–134. doi:10.1016/j.chroma.2016.02.054.
[42] A. Criscuolo, M. Zeller, K. Cook, G. Angelidou, M. Fedorova, Rational selection of reverse phase columns for high throughput LC–MS lipidomics, Chem. Phys. Lipids. 221 (2019) 120–127. doi:10.1016/j.chemphyslip.2019.03.006.
[43] Y.Y. Tyurina, V.A. Tyurin, V.I. Kapralova, K. Wasserloos, M. Mosher, M.W. Epperly, J.S. Greenberger, B.R. Pitt, V.E. Kagan, Oxidative Lipidomics of γ-Radiation-Induced Lung Injury: Mass Spectrometric Characterization of Cardiolipin and Phosphatidylserine Peroxidation, Radiat. Res. 175 (2011) 610–621. doi:10.1667/RR2297.1.
[44] S. Colombo, P. Domingues, M.R. Domingues, Mass spectrometry strategies to unveil modified aminophospholipids of biological interest: mass spectrometry of modified aminophospholipids, Mass Spectrom. Rev. (2018). doi:10.1002/mas.21584.
[45] S. Colombo, G. Coliva, A. Kraj, J.-P. Chervet, M. Fedorova, P. Domingues, M.R. Domingues, Electrochemical oxidation of phosphatidylethanolamines studied by mass spectrometry, J. Mass Spectrom. 53 (2018) 223–233. doi:10.1002/jms.4056.
[46] M.R. Asam, G.L. Glish, Tandem mass spectrometry of alkali cationized polysaccharides in a quadrupole ion trap, J. Am. Soc. Mass Spectrom. 8 (1997) 987–995. doi:10.1016/S1044-0305(97)00124-4.
[47] J. Simões, P. Domingues, A. Reis, F.M. Nunes, M.A. Coimbra, M.R.M. Domingues, Identification of Anomeric Configuration of Underivatized Reducing Glucopyranosyl-glucose Disaccharides by Tandem Mass Spectrometry and Multivariate Analysis, Anal. Chem. 79 (2007) 5896–5905. doi:10.1021/ac070317i.
[48] A. Reis, P. Domingues, A.J.V. Ferrer-Correia, M.R.M. Domingues, Tandem mass spectrometry of intact oxidation products of diacylphosphatidylcholines: evidence for the occurrence of the oxidation of the phosphocholine head and differentiation of isomers, J. Mass Spectrom. 39 (2004) 1513–1522. doi:10.1002/jms.751.
[49] A.H. Morgan, V.J. Hammond, L. Morgan, C.P. Thomas, K.A. Tallman, Y.R. Garcia-Diaz, C. McGuigan, M. Serpi, N.A. Porter, R.C. Murphy, V.B. O'Donnell, Quantitative assays for esterified oxylipins generated by immune cells, Nat. Protoc. 5 (2010) 1919–1931. doi:10.1038/nprot.2010.162.
[50] V.J. Hammond, V.B. O'Donnell, Esterified eicosanoids: Generation, characterization and function, Biochim. Biophys. Acta BBA - Biomembr. 1818 (2012) 2403–2412. doi:10.1016/j.bbamem.2011.12.013.
[51] V.B. O'Donnell, R.C. Murphy, New families of bioactive oxidized phospholipids generated by immune cells: identification and signaling actions, Blood. 120 (2012) 1985–1992. doi:10.1182/blood-2012-04-402826.
[52] S.R. Clark, C.J. Guy, M.J. Scurr, P.R. Taylor, A.P. Kift-Morgan, V.J. Hammond, C.P. Thomas, B. Coles, G.W. Roberts, M. Eberl, others, Esterified eicosanoids are acutely

738 generated by 5-lipoxygenase in primary human neutrophils and in human and murine
739 infection, Blood. 117 (2011) 2033–2043.
740 [53] L.T. Morgan, C.P. Thomas, H. Kühn, V.B. O'Donnell, Thrombin-activated human platelets
741 acutely generate oxidized docosahexaenoic-acid-containing phospholipids via 12-
742 lipoxygenase, Biochem. J. 431 (2010) 141–148. doi:10.1042/BJ20100415.
743 [54] C.P. Thomas, L.T. Morgan, B.H. Maskrey, R.C. Murphy, H. Kuhn, S.L. Hazen, A.H. Goodall,
744 H.A. Hamali, P.W. Collins, V.B. O'Donnell, Phospholipid-esterified Eicosanoids Are
745 Generated in Agonist-activated Human Platelets and Enhance Tissue Factor-dependent
746 Thrombin Generation, J. Biol. Chem. 285 (2010) 6891–6903. doi:10.1074/jbc.M109.078428.
747 [55] A. Yamashita, H. Morikawa, N. Tajima, M. Teraoka, C. Kusumoto, K. Nakaso, T. Matsura,
748 Mechanisms underlying production and externalization of oxidized phosphatidylserine in
749 apoptosis: involvement of mitochondria, Yonago Acta Med. 55 (2012) 11–20.
750 [56] S. Bluml, B. Rosc, A. Lorincz, M. Seyerl, S. Kirchberger, O. Oskolkova, V.N. Bochkov, O.
751 Majdic, E. Ligeti, J. Stockl, The Oxidation State of Phospholipids Controls the Oxidative
752 Burst in Neutrophil Granulocytes, J. Immunol. 181 (2008) 4347–4353.
753 doi:10.4049/jimmunol.181.6.4347.
754 [57] M. Seyerl, S. Blüml, S. Kirchberger, V.N. Bochkov, O. Oskolkova, O. Majdic, J. Stöckl,
755 Oxidized phospholipids induce anergy in human peripheral blood T cells, Eur. J. Immunol. 38
756 (2008) 778–787.
757

Analysis of oxidised and glycated aminophospholipids: complete structural characterisation by C30 liquid chromatography-high resolution tandem mass spectrometry

Highlights

The new highlights are:

- C30 LC-MS allows long- and short-chain oxidation products of APL to be separated
- C30 LC-MS allows glycated APL, oxidised on fatty acids or glucose, to be separated
- C30 LC-MS resolved functional/positional isomers of oxidised and glycoxidised APL
- HCD-MS/MS fragmentation confirmed the identity of each isomer after LC separation